Journal of Medicinal Chemistry

Article

Cite This: J. Med. Chem. 2019, 62, 1468−1483

pubs.acs.org/jmc

Discovery of Novel Transient Receptor Potential Vanilloid 4 (TRPV4) Agonists as Regulators of Chondrogenic Differentiation: Identification of Quinazolin-4(3*H*)-ones and in Vivo Studies on a Surgically Induced Rat Model of Osteoarthritis

Masakazu Atobe,*[,†,▽] Takamichi Nagami,[‡,▽] Shuji Muramatsu,[‡,⊥] Takeshi Ohno,[‡,⊥] Masayuki Kitagawa,[‡,⊥] Hiroko Suzuki,[§] Masashi Ishiguro,[§] Atsushi Watanabe,[∥] and Masashi Kawanishi[†]

[†]Laboratory for Medicinal Chemistry, Pharmaceutical Research Center, [‡]Laboratory for Pharmacology, Pharmaceutical Research Center, and [§]Laboratory for Safety Assessment & ADME, Pharmaceutical Research Center, Asahi Kasei Pharma Corporation, 632-1 Mifuku, Izunokuni, Shizuoka 410-2321, Japan

[∥]Medical Technology & Material Laboratory, Medical Products Development Division, Asahi Kasei Medical Corporation, 632-1 Mifuku, Izunokuni, Shizuoka 410-2321, Japan

Supporting Information

ABSTRACT: Osteoarthritis (OA) is a degenerative disease characterized by joint destruction and loss of cartilage. There are many unmet needs in the treatment of OA and there are few promising candidates for disease-modifying OA drugs, particularly, anabolic agents. Here, we describe the identification of novel quinazolin-4(3*H*)-one derivatives, which stimulate chondrocyte cartilage matrix production via TRPV4 and mitigate damaged articular cartilage. We successfully identified the water-soluble, highly potent quinazolin-4(3*H*)-one derivative **36** and studied its intra-articular physicochemical profile to use in in vivo surgical OA model studies. Compound **36·HCl** provided relief from OA damage in a rat medial meniscal tear (MT) model. Specifically, **36·HCl** dose-dependently suppressed cartilage degradation and enhanced the messenger RNA expression of aggrecan and SOX9 in cartilage isolated from MT-operated rat knees compared with knees treated with vehicle. These results suggest that **36** induces anabolic changes in articular cartilage and consequently reduces OA progression.

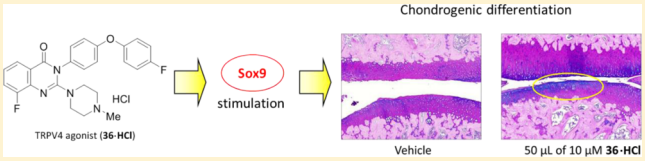

INTRODUCTION

Osteoarthritis (OA) is a degenerative disease that typically affects the elderly and is the most common form of arthritis. OA is characterized by joint destruction and loss of cartilage,[1] the slippery tissue that covers the ends of bones in a joint. Healthy cartilage allows bones to glide over one another and absorbs energy from the shock of physical movement.[2] In OA, the surface layer of cartilage breaks down and wears away, allowing bones under the cartilage to rub together, causing pain, swelling, and loss of motion of the joint. In addition, the joint may lose its normal shape and bone spurs, called osteophytes, may grow on the edges of the joint. Fragments of bone or cartilage can break off and float inside the joint space, causing more pain and damage.[1,2] Various treatments and therapies are available for OA.[3] The existing medications, which are nonsteroidal anti-inflammatory drugs and corticosteroids, are analgesics that help to relieve pain and act on the immune system by blocking the production of compounds that trigger allergic and inflammatory reactions. Some OA treatments also target processes believed to cause the disease.[4] Severe cases of OA are treated with arthroplasty, which involves reconstruction or replacement of the diseased joint and realignment of the joint.[5]

Recent efforts to identify agents that alter the progression of OA have focused on inhibiting the catabolic cascade of cytokines and enzymes[6] or on anabolic factors that may stimulate the repair of cartilage lesions.[7] The targeting of anabolic factors represents an attractive therapeutic approach for OA. In addition, a number of growth factors have been reported to have anabolic effects on cartilage; for example, FGF18 has shown efficacy in preclinical models of traumatic cartilage injury.[8] To our knowledge, however, there are very few reports[9] of the efficacy of small molecules in animal models in which cartilage damage is due to joint instability. Such models are representative of joint failure in OA.

The SRY (sex-related Y)-type high-mobility group box "SOX9" is a transcription factor that is essential for chondrocyte differentiation and chondrocyte-specific gene expression of molecules,[10,11] such as collagen type II,[12] IX,[13] and XI[14] and aggrecan.[15] Sox9 is involved in the expression of SOX5 and SOX6, both of which form a transcriptional complex with SOX9 and control the expression of type II collagen and aggrecan.[16] However, the precise mechanism of SOX9 activation during chondrogenesis is not fully understood. In our previous study, we performed functional gene screening to identify genes that activate SOX9-dependent transcription, using full-length

Received: October 18, 2018
Published: January 10, 2019

DOI: 10.1021/acs.jmedchem.8b01615
J. Med. Chem. 2019, 62, 1468−1483

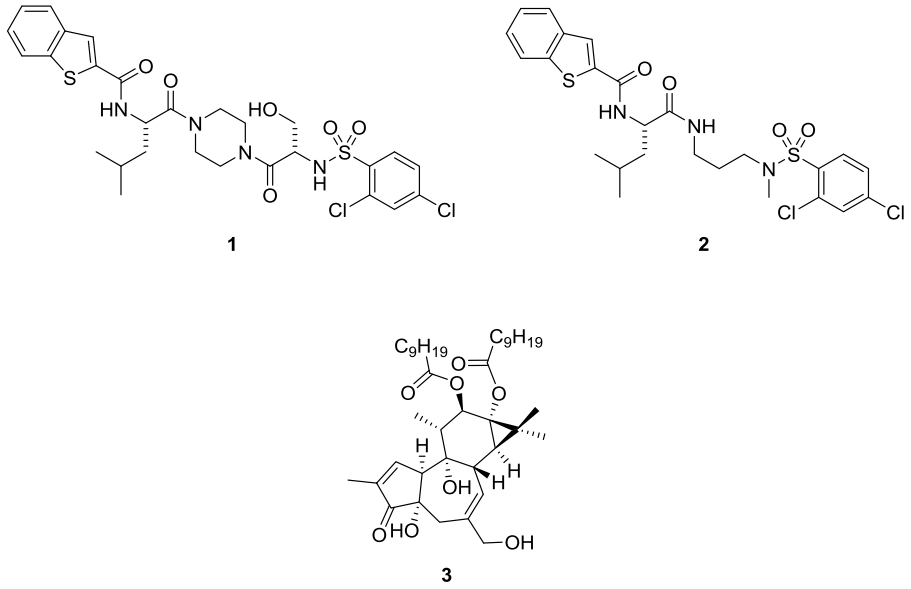

Figure 1. GSK compounds **1** and **2** and 4αPDD **3**.

complementary DNA (cDNA) libraries generated from a murine chondrogenic cell line, ATDC5.[17] In that study, we identified the protein TRPV4 through its effect on SOX9-dependent transcription. Our data suggested that TRPV4 plays an important role in early chondrogenesis. Thus, examining the role of TRPV4 during hypertrophic differentiation in late chondrogenesis would be informative because SOX9 functions as a negative regulator in this process.

TRPV4 is widely expressed in epithelial cells and is found in the brain, endothelium, liver, dorsal root ganglia, bladder, skin, heart, and cartilage.[18] The literature reports the contribution of TRPV4 in several pathological conditions, such as hypotonic hyperalgesia, thermal hyperalgesia, asthma, and neuropathic pain.[19] Several small-molecule inhibitors of TRPV4 have been identified.[20] Notably, researchers at Glaxo Smith Klein (GSK) showed that the piperazine-linked TRPV4 agonist GSK1016790A (**1**) exhibits higher potency and selectivity against TRPV1 than for 4αPDD (**3**), a semisynthetic nontumor promoter phorbol ester (Figure 1).[21] Compound (**2**) with a similar structure but lacking a piperazine ring has also been described.[22] GSK researchers disclosed that the intravenous administration of **1** (Figure 1) led to a dose-dependent reduction in blood pressure, circulatory collapse, and death and concluded that TRPV4 is toxic to humans due to its agonistic modulation of many physiological functions.[23]

Given these advantages and disadvantages of TRPV4 agonists, our aim is to identify a highly potent TRPV4 agonistic modulator with good physicochemical properties for intra-articular administration into exposed joint cartilages. We intend to avoid oral and intravenous administration routes so that the entire body is not exposed to the TRPV4 agonistic modulator. We first confirmed whether GSK-patented compound **1** or phorbol ester **3** are appropriate therapeutic compounds. Our results suggested that the high lipophilicity and large molecular weights of **1** and **3** make them unsuitable for use in in vivo validation studies. Here, we describe the optimization of our novel TRPV4 agonist and its in vivo evaluation.

RESULTS AND DISCUSSION

Optimization of Quinazolin-4(3*H*)-one 4 for Use in in Vivo Studies. High-throughput screening using SOX9 reporter assays with ATDC5 cells and our 350 000 inhouse compound library identified 24 hit compounds (0.007% hit rate). Quinazolin-4(3*H*)-one **4** showed moderate SOX9 reporter activity (Figure 2). The potency of **4** was canceled with

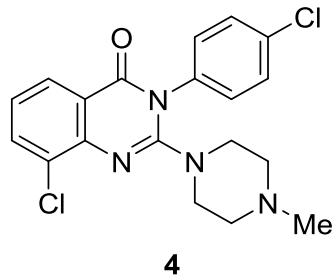

Figure 2. HTS hit compound **4**.

ruthenium red, which is TRPV4 antagonist; thus, SOX9 reporter activity derives from TRPV4 agonistic activity. TRPV4 conducts Ca^{2+} and Na^{+} across the plasma membrane of various cell types with a 6:1 selectivity under physiological conditions,[24] which normally enhances cellular excitability. Consequently, compound **4** was tested for activity using the TRPV4 Ca^{2+} assay (EC_{max}[25] 19% at 10 μM). Several sulfonamide-type hit compounds showed moderate SOX9 reporter activity, but all compounds showed relatively high lipophilic profiles and had structures similar to **1** and **2** (structures not shown). We therefore chose compound **4** for further optimization to improve its TRPV4 agonistic activity and solubility in aqueous buffer to work toward an injectable compound.

Structure–activity relationship (SAR) studies of **4** were carried out to obtain more potent compounds (Table 1). We first conducted SAR studies on the phenyl ring. Compound **5** (R^4 = Me) showed moderate activity whereas **6** (R^5 = Me) and **7** (R^6 = Me) showed no potency, thereby directing us to R^4 as a potential position for other substituents. Compound **8** (R^4 = CO_2Et) showed activity similar to that of **5**. The replacement of

DOI: 10.1021/acs.jmedchem.8b01615
J. Med. Chem. 2019, 62, 1468–1483

Table 1. Initial Optimization of HTS Hit Compound 4

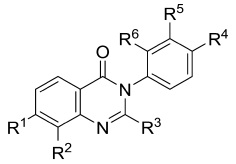

Cpd.	R^1	R^2	R^3	R^4	R^5	R^6	SOX 9 reporter (10 μM)	SOX 9 reporter ECmax	hTRPV4 Ca^{2+} EC_{50}
4	-H	-Cl	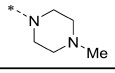	Ar	-H	-H	19.9%		
5	-H	-Cl	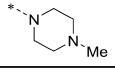	-Me	-H	-H	9.0%		
6	-H	-Cl	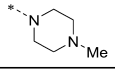	-H	-Me	-H	1.5%		
7	-H	-Cl	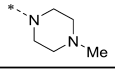	-H	-H	-Me	0.4%		
8	-H	-Cl	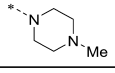	$-CO_2Et$	-H	-H	29.4%		
9	-H	-F	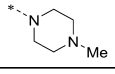	$-CO_2Et$	-H	-H		625 nM	920 nM
10	-H	-H	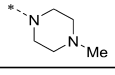	-OMe	-H	-H	13.2%		
11	-H	-Br	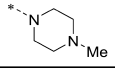	$-CO_2Et$	-H	-H	7.8%		
12	-H	-OMe	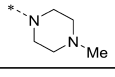	-Me	-H	-H	1.3%		
13	-H	-F	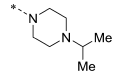	$-CO_2Et$	-H	-H	1.9%		
14	-H	-F	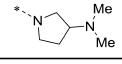	$-CO_2Et$	-H	-H	2.2%		
15	-H	-F	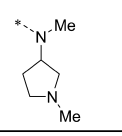	$-CO_2Et$	-H	-H	0.3%		
16	-F	-H	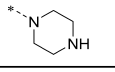	-OMe	-H	-H	1.8%		
17	-F	-H	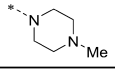	-OMe	-H	-H	42.2%	5000 nM	4700 nM
18	-F	-H	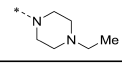	-OMe	-H	-H	41.0%		12200 nM
19	-F	-H	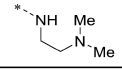	-OMe	-H	-H	0%		
20	-F	-H	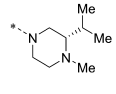	$-CF_3$	-H	-H		5000 nM	>30000 nM

DOI: 10.1021/acs.jmedchem.8b01615
J. Med. Chem. 2019, 62, 1468−1483

Table 1. continued

21	-F	-H	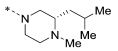	$-CF_3$	-H	-H	0.9%		
22	-F	-H	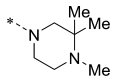	$-CF_3$	-H	-H	5.0%	10000 nM	>30000 nM
23	-F	-H	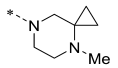	$-CF_3$	-H	-H	1.2%		
24	-F	-H	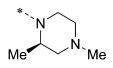	$-CF_3$	-H	-H	41.7%		10000 nM
25	-F	-H	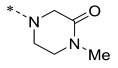	-F	-H	-H	1.8%		
26	-H	-F	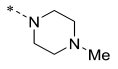	$-CF_3$	-H	-H		2500 nM	1444 nM
27	-H	-F	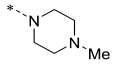		-H	-H		2500 nM	910 nM
28	-H	-F	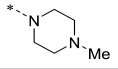	$-OCF_3$	-H	-H		625 nM	280 nM
29	-H	-F	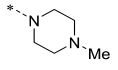	$-SCF_3$	-H	-H		156 nM	200 nM

Cl by F at the R^2 position improved activity and gave an EC_{50} of 920 nM in the Ca^{2+} assay. We next studied the SAR of the R^2 position and observed decreased activity for compounds **10** (R^2 = H), **11** (R^2 = Br), and **12** (R^2 = OMe). Replacement of the piperazine unit to give compounds **13**, **14**, and **15** also resulted in decreased potency. Further exploration of potential substituents on the piperazine unit in compounds **16**–**25** also resulted in reduced or lost activity. In contrast, the optimization of R^4 in compounds **26**, **27**, and **28** resulted in good potency (2500, 2500, and 625 nM, respectively) and **29** showed excellent activity at 156 nM.

We next investigated potentially important positions on the quinazolin-4(3*H*)-one core of **28** using a fluorine scanning strategy[26] (Table 2). Compounds **30** (R^1 = F) and **31** (R^2 = F) showed moderate activity (1250 and 2500 nM, respectively).

Table 2. Results of the Fluorine Scanning Strategy

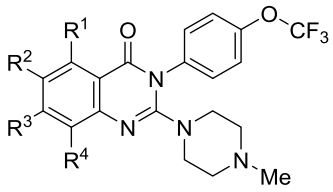

cpd.	R^1	R^2	R^3	R^4	SOX9 reporter assay EC_{max} (nM)	hTRPV4 Ca^{2+} EC_{50} (nM)	hTRPV1 Ca^{2+} (10 μM) (%)
28	-H	-H	-H	-F	625	280	2.2
30	-F	-H	-H	-H	1250	1180	3.7
31	-H	-F	-H	-H	2500	2060	5.0
32	-H	-H	-F	-H	625	663	6.2

Compound **32** (R^3 = F) showed activity similar to that observed using the SOX9 reporter assay (625 nM), and its activity in the hTRPV4 Ca^{2+} assay was slightly lower than that of **28**. Thus, R^4 is the best position for a fluorine atom.

We attempted further optimization using rapid solid-phase synthesis by replacing the CF_3 with other substituted groups. The results are summarized in Table 3. Compound **33**, bearing a tetrahydropyran group, showed slightly less activity than **34** but had good solubility and a lower protein binding ratio than that of **34**. Compound **35** exhibited significantly increased potency (EC_{max}: 39 nM in the SOX9 reporter assay). Compound **36**, bearing a 4-phenyl group, showed the best SOX9 reporter assay activity and hTRPV4 Ca^{2+} assay results. Compound **36** was inactive against TRPV1 channels, the TRP superfamily member closest to TRPV4 on the basis of sequence homology. We tested **36** using the Ames test and ATP assay using HL-60 cell viability because these cells provide a sensitive assay for evaluating the cytotoxicities of compounds.[27] No toxicity was observed. Also, **36** exhibited good solubility in saline solution and a moderate protein binding ratio. Therefore, **36** was chosen as the most promising compound for testing in an animal OA model.

Evaluation of Compounds Using the Human Articular Chondrocyte (NHAC) Cell Assay. Next, we screened selected compounds for in vivo study by evaluating their cell activities using the normal human articular chondrocyte (NHAC) cell assay.[28] Chondrocytes are specialized cells that produce and maintain the extracellular matrix of cartilage and are the only cellular component of cartilage. The results are shown in Figure 3. Compound **2** was not active below 500 nM, whereas **29** and **36** showed sufficient activity to generate chondrocyte extracellular matrix stained by Alcian blue, suggesting their possible chondrogenesis activity. It is noteworthy that **36**

DOI: 10.1021/acs.jmedchem.8b01615
J. Med. Chem. 2019, 62, 1468−1483

Table 3. Final Optimization Results

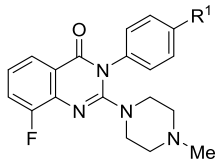

	R^1	SOX9 rep ECmax	hTRPV4 Ca^{2+} EC_{50}	hTRPV1 Ca^{2+} (10 μM)	Protein Bind (%)	Solubility (Saline) μg/ml
28	-OCF_3	625 nM	280 nM	2.2%	17.6%	951
29	-SCF_3	156 nM	200 nM	3.1%	4.7%	952
33	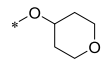	2500 nM	870 nM	8.7%	29.7%	1107
34	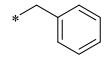	312 nM	670 nM	1.5%	4.4%	553
35	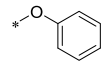	39 nM	125 nM	0.6%	1.7%	745
36	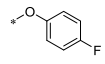	20 nM	60 nM	0.6%	1.7%	743
1		ND	49 nM	ND	0.2%	0
2		312 nM	740 nM	ND	0.003%	3.6

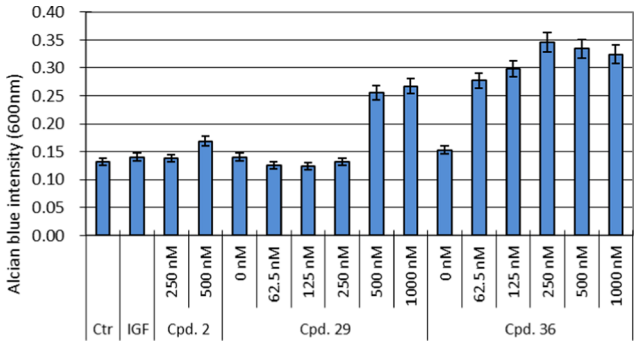

Figure 3. Human chondrocyte assay results following 30 min stimulation with TRPV4 agonists.

showed activity at 62.5 nM, as determined by the Alcian blue intensity, which is the highest activity and thus the highest potency of the tested compounds.

Measurement of the Concentrations of 1, 29·HCl, and 36·HCl in Articular Cartilage. On the basis of our concept of an ideal TRPV4 agonist for treating OA, the three drug candidates were injected into articular joints directly (SI Figure 1). Injected TRPV4 agonist quickly stimulates ion channels to activate chondrocytes to produce extracellular matrix. The matrix is transferred to the systemic blood and quickly eliminated from the body. This "soft-drug" concept requires short-term action and not long residency in the articular cartilage, as indicated by our cell studies. We therefore prepared **29·HCl** and **36·HCl** for the injection and monitored the pharmacokinetics (PK) of **1**, **29·HCl**, and **36·HCl** in joints by injecting the compounds into the knee joints of normal rats. After euthanizing the rats, the joints were washed by injecting saline and the synovial fluid lavage (SFL) was collected. The concentration of each test compound in the lavage from the articular joint was measured by liquid chromatography with tandem mass spectrometry and then converted to the concentration in the joint using the ratio of the total protein concentration in the lavage. The analytical quantitation limits of **1**, **29·HCl**, and **36·HCl** were 0.3, 1, and 1 nmol/L, respectively, as shown in Figure 4. GSK compound **1** showed long-term PK

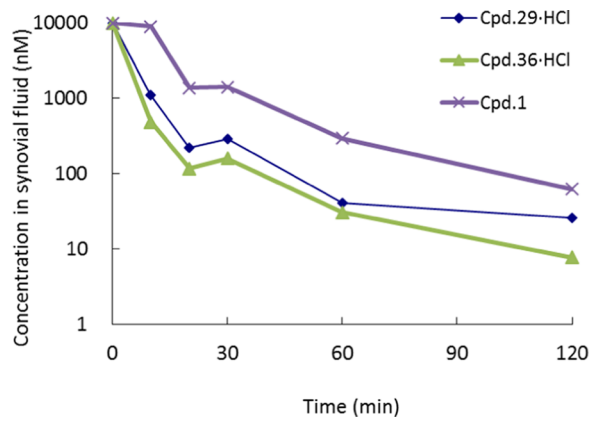

Figure 4. Concentration study in synovial fluid.

due to its high lipophilicity. The residence time of a drug in the joint was derived from protein binding against albumin.[29] There is an equilibrium between serum and joint cartilage due to passive diffusion. Unbound drugs can permeate the cell membrane or cartilage and should have low lipophilicities, and thus GSK compound **1** does not meet our criteria (Figure 4). We then performed the same assay with **29·HCl** and **36·HCl**, and the results are shown Figure 4. Compound **36·HCl** provided an ideal PK plot, quickly leaving the joint cavity (within 30 min),

DOI: 10.1021/acs.jmedchem.8b01615
J. Med. Chem. 2019, 62, 1468−1483

and thus **36·HCl** exhibited the most promising profile for surgical OA model studies.

Induction of OA in an MT Model and Drug Treatment. Osteoarthritis models have classically been categorized into spontaneous and induced models.[30−36] For simplicity, the models have been grouped into two basic classes of OA: primary osteoarthritis (POA) and post-traumatic osteoarthritis (PTOA, a subcategory of secondary OA). A large number of surgically induced OA models have been reported and include the medial meniscal tear (MT) model.[37] There is a strong association between meniscal damage and cartilage loss, making the rat MT model an attractive preclinical model for degenerative joint diseases.

We evaluated whether our TRPV4 agonist **36·HCl** can facilitate relief from cartilage damage caused by OA by testing the efficacy of **36·HCl** in an in vivo rat MT model. In this model, a full-thickness cut in the medial meniscus leads to joint instability and progressive development of OA characterized by proteoglycan loss, cartilage fibrillation, chondrocyte death, eventual damage to the subchondral bone, and formation of osteophytes.[31,38]

The results of the rat MT-model studies are shown in Figure 5. Operated knees intra-articularly received a 50 μL injection of 0, 5, or 10 μM of **36·HCl** twice weekly for 3 weeks. Saline was used as the vehicle. No deaths occurred, and no obvious systemic effects of **36·HCl** treatment were observed by gross visual inspection of the animals. No significant differences in final body weights were noted among the MT-operated groups of rats.

Histological observation showed that the sham-operated animals exhibited no cartilage degeneration whereas the vehicle-treated animals showed significant cartilage degeneration. The anabolic effects of **36·HCl** were quantified by measuring the length of the damaged area. Collapse of articular cartilage into the tibial epiphysis was occasionally observed. (Figure 5a). Intra-articular injection of **36·HCl** resulted in a dose-dependent decrease in the length of the damaged area (Figure 5b,c).

In addition to determining the anabolic effects of **36·HCl** at the articular surface, medial sections were stained with either Safranin O/Fast Green or AB-PAS and observed microscopically (Figure 6). Little or no staining was observed following vehicle administration. In contrast, the administration of 10 μM **36·HCl** resulted in an area stained by both Safranin O/Fast Green and AB-PAS. Histological analysis of the joint sections indicated that **36·**HCl-induced newly generated extracellular matrix. The anabolic effects observed with **36·HCl** are likely due to its TRPV4 agonistic activity increasing the concentration of SOX9 in the joint.

Next, we measured aggrecan and SOX9 messenger RNA (mRNA) expression. A dose-dependent increase in the mRNA expression of aggrecan (Figure 7a) and SOX9 (Figure 7b) was observed in the cartilage of rat knee joints injected intra-articularly with **36·HCl** 21 days after MT surgery. These changes in mRNA expression are likely associated with the decreased pathological damage of cartilage and suggest that small-molecule **36·HCl** induces anabolic changes in articular cartilage and thus reduces OA progression. A detailed mechanism for these effects is currently not available but the data are consistent with the in vivo observations that **36·HCl** stimulates an increase in SOX9 and then increases the production of extracellular matrix via chondrocyte differentiation.

In this report, we demonstrated that **36·HCl** promoted extracellular matrix production in chondrocytes. Intra-articular injection of **36·HCl** reduced cartilage degradation in rat MT models. **36·HCl** was administrated twice a week for 3 weeks starting 1 week after MT surgery and dose-dependently reduced the erosion of tibial plateau cartilage. Although **36·HCl** rapidly leaves the joint cavity, mRNA expression of aggrecan and the transcription factor SOX9 was enhanced in knee cartilage isolated from **36·HCl**-treated rat MT models. These results suggest that **36·HCl** may promote chondrocyte differentiation and extracellular matrix production, thereby reducing cartilage degradation in rat OA models.

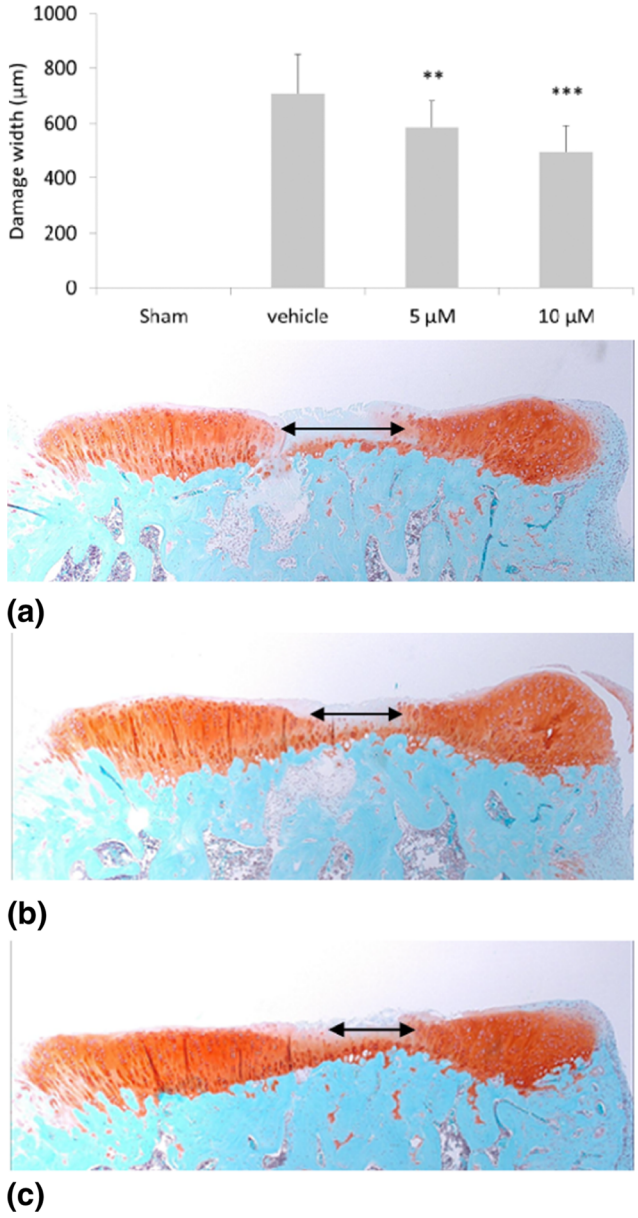

Figure 5. Width of damaged medial tibial cartilage in a rat MT model, mean ± SE, n = 5 (sham), n = 15 (vehicle), n = 14 (5 μM), and n = 15 (10 μM) (p value *: $p < 0.05$ **: $p < 0.01$ ***: $p < 0.001$, by Dunnett's test). (a) vehicle. (b) 5 μM. (c) 10 μM. Figure 5 Intra-articular injection of **36·HCl** resulted in reduced cartilage lesion area in a rat MT model. Rats were subjected to meniscal tear and treatment with either the vehicle alone or with vehicle containing **36·HCl** at different concentrations. The width of the damaged area following treatment with each concentration of **36·HCl**. Safranin O and Fast Green-stained coronal sections of the medial tibial plateau of rats treated with vehicle, 5 μM (b), and 10 μM (c) of **36·HCl**.

DOI: 10.1021/acs.jmedchem.8b01615
J. Med. Chem. 2019, 62, 1468−1483

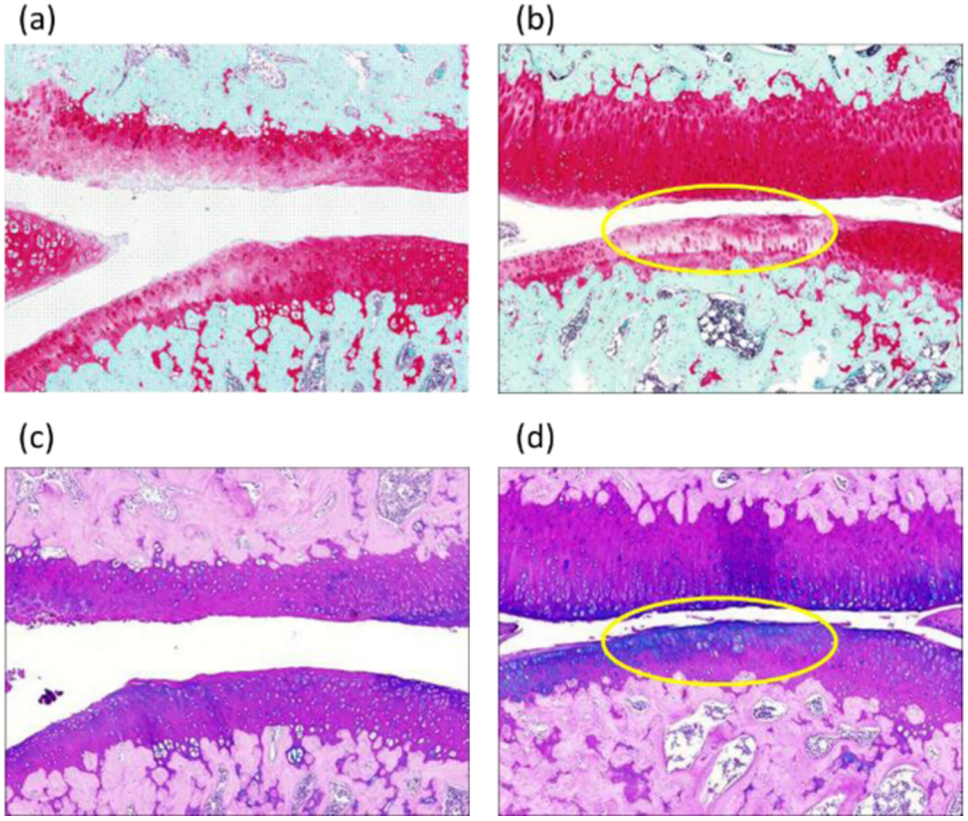

Figure 6. Medial sections, Safranin O, and Fast Green staining following treatment with vehicle (a), 10 μM of **36·HCl** (b); AB-PAS staining following treatment with vehicle (c), 10 μM of **36·HCl** (d).

CHEMISTRY

The quinazolin-4(3*H*)-one derivatives **4**–**9**, **11**–**15**, **26**–**29**, and **33**–**36** were synthesized by solid-phase aza-Wittig-mediated annulation methods[39,40] on an e-DOMINO solid-phase synthesizer invented by us[41] (Scheme 1). Azidation of the easily available anthranilic acid **37** under Sandmeyer conditions gave ortho azido benzoic acid **38** in 99% yield. Compound **38** was readily coupled using typical amidation conditions with dicyclohexylcarbodiimide to afford the corresponding polymer-bound *ortho*-azide ester **39**. Iminophosphorane was synthesized by exposing **39** to PPh_3 in tetrahydrofuran at room temperature, followed by isocyanate, to give carbodiimide **41**. Finally, treatment with various piperazine derivatives, followed by intramolecular cyclization and simultaneous cleavage from the resin, provided the quinazolin-4(3*H*)-ones **4**–**9**, **11**–**15**, **26**–**29**, and **33**–**36**. For the use of in vivo studies, **29** and **36** were treated with 1 M HCl in MeOH solution to give the corresponding HCl salts, **29·HCl** and **36·HCl**.

Compounds **10**, **17**–**19**, and **30**–**32** were synthesized using a liquid-based synthetic route, as shown in Scheme 2.[42] Isatoic anhydrides **45a** and **45b** were prepared from anthranilic acids **44a** and **44b** with treatment of triphosgene. Other isatoic anhydrides **45c**–**e** are commercially available. Treatment of isatoic anhydrides (**45**) with aniline **46a** and **46b**, followed by cyclization with thiocarbonyldiimidazole, afforded the thiocarbonyl 4(1*H*)-quinazolinone **48**. Chlorination of **48** with sulfuryl chloride gave 2-chloro-4(3*H*)-quinazolinone **49**, which was treated with the amines *N*-methylpiperazine **43a**, and 2-*N*,*N*-dimethylaminoethylamine **43e** to give the corresponding 2-position-substituted quinazolin-4(3*H*)-ones **10**, **17**–**19**, and **30**–**32**.

We next prepared various substituted derivatives of the piperazine ring using **49c** and **49d** as the common intermediates. Piperazines **51a**–**f** were aminated, followed by deprotection and *N*-methylation, with typically good yields (Scheme 3).

CONCLUSIONS

We have identified novel quinazolin-4(3*H*)-one derivatives that exhibit anabolic activity toward chondrogenic differentiation and provide relief against articular cartilage damage via TRPV4 agonistic stimulation. Highly potent quinazolin-4(3*H*)-one **36** exhibited good solubility, a promising physicochemical profile, and high potency in an NHAC cell assay. Intra-articular injection of **36·HCl** suppressed OA progression in rat MT models. Furthermore, **36·HCl** enhanced the mRNA expression of aggrecan and SOX9 in tibial cartilage isolated from MT rats. These findings suggest that TRPV4 agonist **36·HCl** stimulates chondrocyte anabolic changes and helps suppress OA progression. Our novel approach of promoting new cartilage formation by using a TRPV4 agonist holds promise as a treatment approach for OA. In addition, compound **36·HCl** is a promising candidate of the disease-modifying OA drug.

EXPERIMENTAL SECTION

General Chemistry Information. NMR spectra were run at 300 MHz on JEOL Co. and at 400 and 600 MHz on Varian Co. As a solvent, deuterated chloroform was used, unless specifically described otherwise. For measurement of chemical shift, tetramethylsilane (TMS) was employed as an internal standard. Chemical shifts (δ) are expressed in ppm. Data for proton spectra are reported as follows: chemical shift (multiplicity [singlet (s), doublet (d), triplet (t), and multiplet (m)], coupling constants [Hz], and integration). Carbon spectra were recorded with complete proton decoupling, and the

DOI: 10.1021/acs.jmedchem.8b01615
J. Med. Chem. 2019, 62, 1468–1483

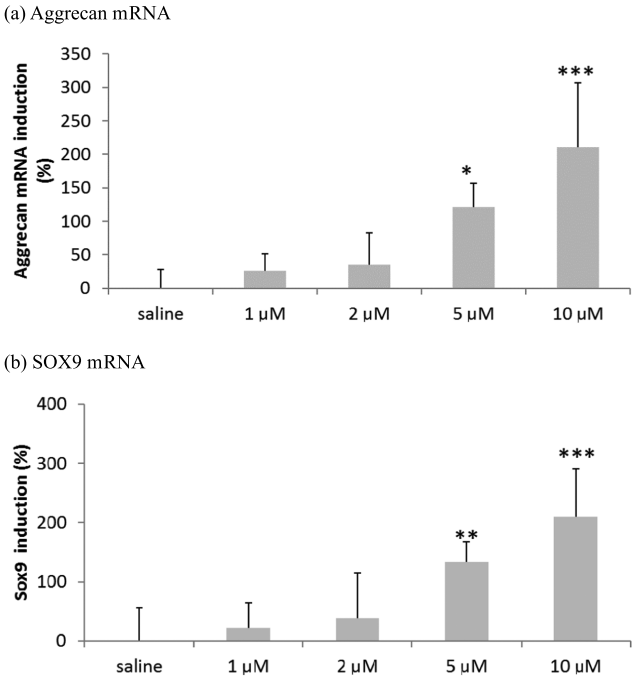

Figure 7. 36·HCl-induced expression of mRNA related to cartilage matrix in isolated medial tibial cartilage from MT rats. Aggrecan (a) and SOX9 (b). The ordinate shows induction ratio (%), mean ± SE, $n = 5$ (saline), $n = 8$ (1 μM), $n = 8$ (2 μM), $n = 7$ (5 μM), and $n = 8$ (10 μM), (p value *: $p < 0.05$ **: $p < 0.01$ ***: $p < 0.001$, by Dunnett's test). Intra-articular injection of **36·**HCl-induced chondrogenesis and promoted repair of cartilage lesions in rats with MT-induced OA. Rats were subjected to meniscal tear and treatment with either vehicle alone or vehicle containing **36·HCl**, as described under concentration.

chemical shifts are reported in ppm. As a mass spectrometer, the quadrupole type mass spectrometer, UPLC/SQD system, manufactured by Waters Company was used, and ionization was carried out on the basis of an electrospray method (ESI) for the measurement. The liquid chromatography instrument used was Acquity Ultra Performance LC system. As a separation column, ACQUITY UPLC BEH (C_{18} 2.1 × 50 mm 1.7 μM, Waters Company) was used. With respect to the examples and the reference examples in which specific descriptions are given for LC condition, the measurements were carried out by using any one of the above described apparatuses and in accordance with the following solvent condition. In addition, m/z indicates mass spectrum data (M + H). Flow rate: 0.6 mL/min. Solvent: solution A = water including 0.1% (v/v) acetic acid, solution B = acetonitrile including 0.1% (v/v) acetic acid. From 0 to 2 min: linear gradient from [solution A 95% + solution B 5% (v/v)] to [solution A 10% + solution B 90% (v/v)]. From 2 to 2.5 min: linear gradient from [solution A 10% + solution B 90% (v/v)] to [solution A 2% + solution B 98% (v/v)]. From 2.5 to 2.6 min: linear gradient from [solution A 2% + solution B 98% (v/v)] to [solution A 95% + solution B 5% (v/v)]. From 2.6 to 3.2 min: maintained at [solution A 95% + solution B 5% (v/v)]. Compound purity was determined using HPLC and is ≥95% for all test compounds.

Solid-Phase Synthesis of the Quinazolin-3-one Derivatives (4−9, 11−15, 26−29, and 33−36). *Preparation of Polymer-Bound ortho-Azide Ester.* Solution of carboxylic acid **38a−d** (2.5 equiv) in CH_2Cl_2 (3 mL), HOBt (3.5 equiv) in CH_2Cl_2 (2 mL), DIEA, and DIC (7.0 equiv) were added to a suspension of Wang resin in CH_2Cl_2 suspension with a 10 mL syringe and then agitated at RT for 48 h with an IKA shaker. Thereafter, the reaction mixture was washed with each solvent in the following order, respectively: MeOH (3 mL × 3), CH_2Cl_2 (3 mL × 3), MeOH (3 mL × 3), DMF (3 mL × 3), MeOH (3 mL × 3), and CH_2Cl_2 (3 mL × 3), with E-DOMINO apparatus, and then dried in reduced pressure to give the desired product.

Staudinger Reaction Step. A solution of PPh_3 (5.0 equiv) in THF (4.0 mL) was added to the resin in a 10 mL syringe and then agitated at RT for 16 h. Thereafter, the reaction mixture was washed with each solvent in the following order: three times of a sequence of THF (3 mL

Scheme 1. Polymer-Supported Synthesis of Quinazolin-4(3*H*)-one Derivatives 4−9, 11−15, 26−29, and 33−36[a]

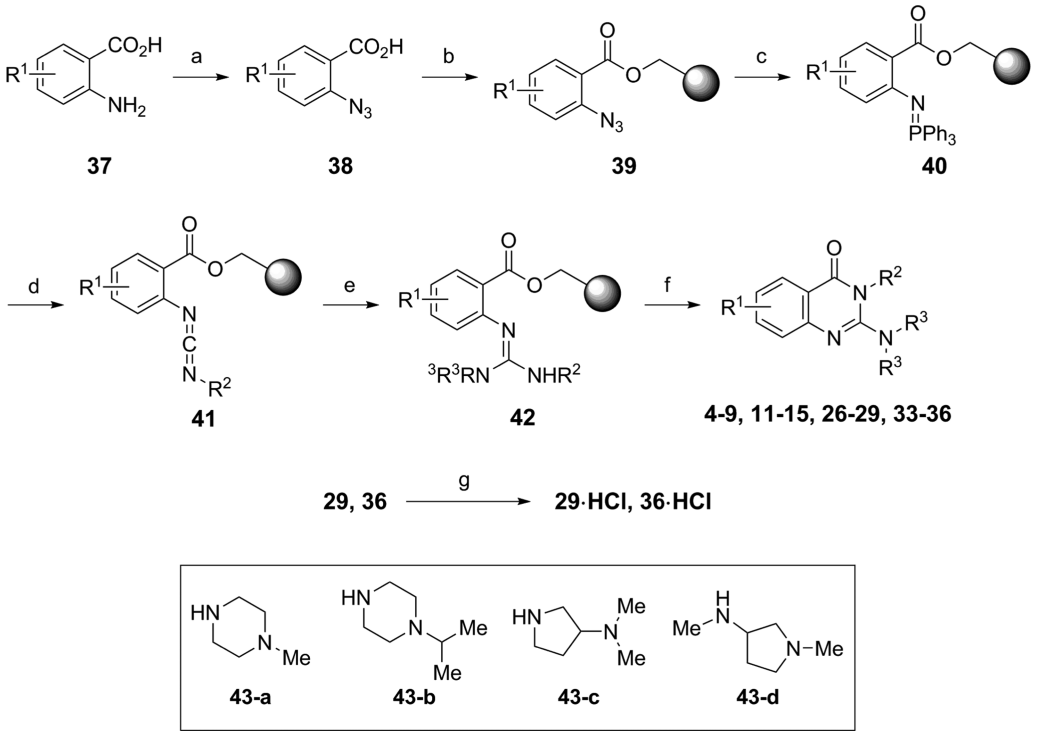

[a]Reagents and conditions: (a) $NaNO_2$, $HCl_{(aq)}$; then NaN_3; (b) Wang resin, DIC, HOBt, DIEA, CH_2Cl_2, rt; (c) PPh_3, THF, rt; (d) R_2NCO, CH_2Cl_2, rt; (e) **43a−d**, CH_2Cl_2, rt; (f) MeOH, 60 °C; (g) 1 M HCl in MeOH.

DOI: 10.1021/acs.jmedchem.8b01615
J. Med. Chem. 2019, 62, 1468−1483

Scheme 2. Synthesis of Quinazolin-4(3*H*)-one Derivatives 10, 17−19, and 30−32[a]

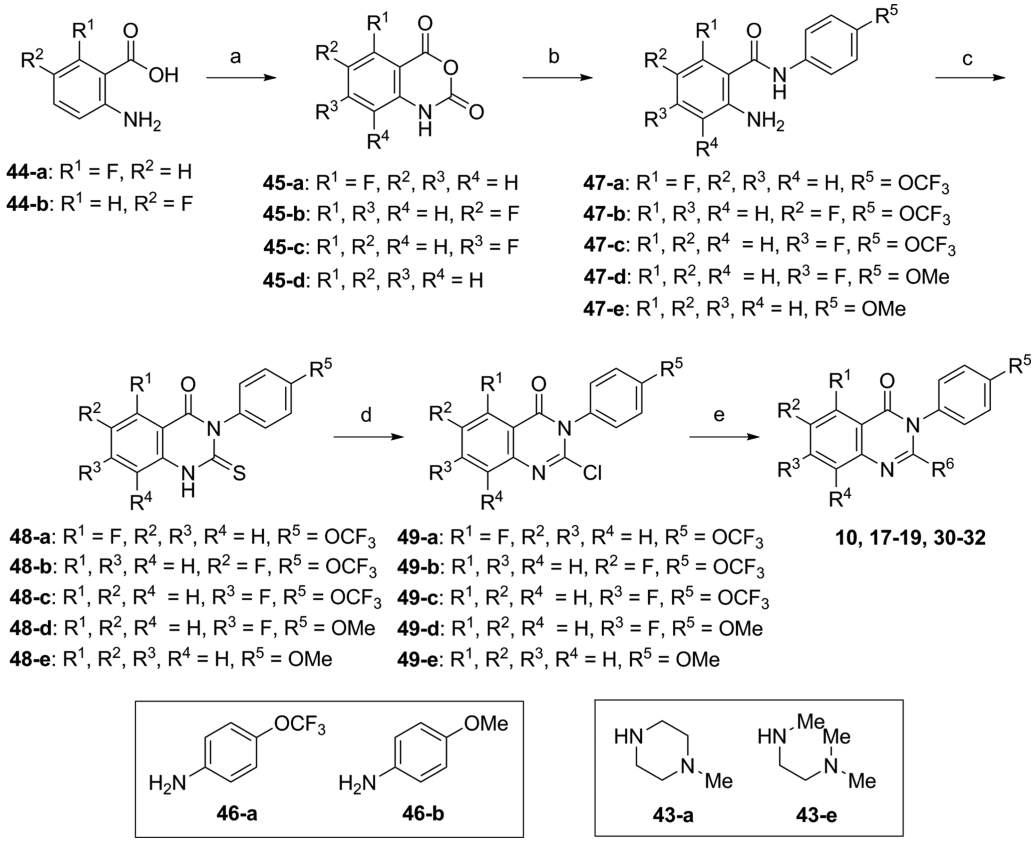

[a]Reagents and conditions: (a) Triphosgene, THF, 0 °C; (b) *p*-anisidine **46a** or **46b**, toluene, reflux; (c) in the case of **49a−d**: 1,1′thiocarbonyldiimidazole, THF, RT or in the case of **49e**: CS_2, NaOH, EtOH, reflux; (d) SO_2Cl_2, $CHCl_3$, reflux; (e) **43a**/**e**, DMSO, 125 °C.

Scheme 3. Synthesis of Quinazolin-4(3*H*)-one Derivatives 16 and 20−25[a]

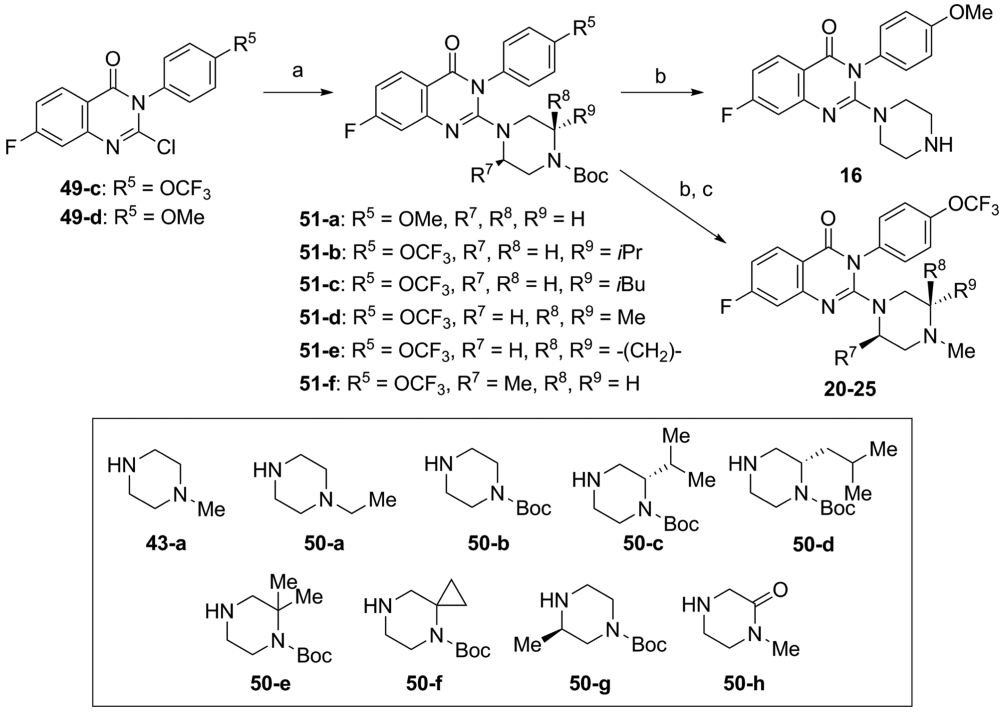

[a](a) **43a** and **50a−h**, DMSO, 125 °C; (b) TFA, CH_2Cl_2, rt; (c) $HCHO_{(aq)}$, $NaBH(OAc)_3$, CH_2Cl_2, rt.

DOI: 10.1021/acs.jmedchem.8b01615
J. Med. Chem. 2019, 62, 1468−1483

× 3), toluene (3 mL × 3), CH_2Cl_2 (3 mL × 3), and hexane (3 mL × 3) with E-DOMINO apparatus, and then dried in reduced pressure to give the desired product.

Aza-Wittig Reaction Step. A solution of isocyanate (5.0 equiv) in CH_2Cl_2 (0.3 mL) was added to the resin in a 10 mL syringe and then agitated at RT for 16 h. Thereafter, the reaction mixture was washed with each solvent in the following order: two times of a sequence of THF (3 mL × 3), toluene (3 mL × 3), CH_2Cl_2 (3 mL × 3), and hexane (3 mL × 3) with E-DOMINO apparatus, and then dried in reduced pressure to give the desired product.

Quinazolin-4(3H)-one-ring Formation Step. A solution of amine (0.6 equiv) in CH_2Cl_2 (0.2 mL) was added to a suspension of the resin in hexane: CH_2Cl_2 = 0.5 mL: 1.5 mL, and the reaction mixture was agitated at 55 °C for 5 h, then agitated at RT for 16 h. The reaction mixture was washed with CH_2Cl_2 (3 mL × 3) and MeOH (3 mL × 3), and the organic layer was evaporated with nitrogen blow down and dried in reduced pressure to give the Quinazolin-3-one (**4**−**9**, **11**−**15**, **26**−**29**, **33**−**36**). All compounds' yields and characteristic data are shown below.

8-Chloro-3-(4-chlorophenyl)-2-(4-methylpiperazin-1-yl)-quinazolin-4(3*H*)-one (4). Yield: 9.6 mg, ^{1}H NMR (400 MHz, DMSO-d_6) δ 8.04 (d, 1H, J = 7.5 Hz, Ar), 7.83 (d, 1H, J = 7.5 Hz, Ar), 7.60−7.55 (m, 4H, Ar), 7.50−7.45 (m, 4H, Ar), 7.29 (dd, 1H, J = 7.5, 7.5 Hz, Ar), 3.27 (br t, 4H, J = 5.0 Hz, CH), 2.29 (br t, 4H, J = 5.0 Hz, CH), 2.24 (s, 3H, NMe); ^{13}C NMR (100.6 MHz, $CDCl_3$) δ 163.05 (C═O), 153.85 (*ipso*-Ar), 144.57 (*ipso*-Ar), 135.83 (*ipso*-Ar), 134.67 (Ar), 133.97 (*ipso*-Ar), 130.26 (Ar), 128.80 (Ar), 125.46 (Ar), 124.34 (Ar), 120.19 (*ipso*-Ar), 53.49 (CH_2), 48.07 (CH_2), 44.52 (CH_3); MS (ESI) m/z 390 [$(M + H)^+$], RT, 0.96 min; purity, 100% (ELSD), 100% (PDA).

8-Chloro-2-(4-methylpiperazin-1-yl)-3-(*p*-tolyl)-quinazolin-4(3*H*)-one (5). Yield: 7.2 mg, ^{1}H NMR (400 MHz, DMSO-d_6) δ 7.94 (dd, 1H, J = 8.0, 1.0 Hz, Ar), 7.87 (dd, 1H, J = 8.0, 1.0 Hz, Ar), 7.36−7.29 (m, 4H, Ar), 7.26 (dd, 1H, J = 8.0, 8.0 Hz, Ar), 3.12 (dd, 4H, J = 8.0, 8.0 Hz, CH), 2.54 (s, 3H, NMe), 2.38 (s, 3H, Me), 2.11−2.02 (m, 4H, CH); MS (ESI) m/z 370 [$(M + H)^+$], RT, 0.92 min; purity, 100% (ELSD), 100% (PDA).

8-Chloro-2-(4-methylpiperazin-1-yl)-3-(*m*-tolyl)-quinazolin-4(3*H*)-one (6). Yield: 7.8 mg, ^{1}H NMR (400 MHz, DMSO-d_6) δ 7.94 (dd, 1H, J = 8.0, 1.0 Hz, Ar), 7.87 (dd, 1H, J = 8.0, 1.0 Hz, Ar), 7.40 (dd, 1H, J = 8.0, 8.0 Hz, Ar), 7.30−7.23 (m, 4H, Ar), 3.13 (dd, 4H, J = 8.0, 8.0 Hz, CH), 2.54 (s, 3H, NMe), 2.36 (s, 3H, Me), 2.09−2.00 (m, 4H, CH); MS (ESI) m/z 370 [$(M + H)^+$], RT, 0.93 min; purity, 100% (ELSD), 100% (PDA).

8-Chloro-2-(4-methylpiperazin-1-yl)-3-(*o*-tolyl)-quinazolin-4(3*H*)-one (7). Yield: 7.2 mg, ^{1}H NMR (400 MHz, DMSO-d_6) δ 7.96 (dd, 1H, J = 8.0, 1.0 Hz, Ar), 7.90 (dd, 1H, J = 8.0, 1.0 Hz, Ar), 7.43−7.33 (m, 4H, Ar), 7.30 (dd, 1H, J = 8.0, 8.0 Hz, Ar), 3.32−3.14 (m, 2H, CH), 3.08−2.99 (m, 2H, CH), 2.54 (s, 3H, NMe), 2.07−1.96 (m, 4H, CH). 2.06 (s, 3H, Me); MS (ESI) m/z 370 [$(M + H)^+$], RT, 0.94 min; purity, 100% (ELSD), 99% (PDA).

Ethyl 4-(8-Chloro-2-(4-methylpiperazin-1-yl)-4-oxoquinazolin-3(4*H*)-yl)-benzoate (8). Yield: 8.5 mg, ^{1}H NMR (400 MHz, DMSO-d_6) δ 8.11−8.09 (m, 1H, Ar), 8.09−8.06 (m, 1H, Ar), 7.96 (dd, 1H, J = 8.0, 1.5 Hz, Ar), 7.90 (dd, 1H, J = 8.0, 1.5 Hz, Ar), 7.67−7.65 (m, 1H, Ar), 7.65−7.63 (m, 1H, Ar), 7.29 (dd, 1H, J = 8.0 Hz, Ar), 4.36 (q, 2H, J = 7.0 Hz, CH_2), 3.10 (dd, 4H, J = 4.0, 4.0 Hz, CH), 2.12−2.00 (m, 4H, CH), 2.06 (s, 3H), 1.36 (t, 3H, J = 7.0 Hz, CH_3); MS (ESI) m/z 428 [$(M + H)^+$], RT, 1.01 min; purity, 100% (ELSD), 95% (PDA).

Ethyl 4-(8-Fluoro-2-(4-methylpiperazin-1-yl)-4-oxoquinazolin-3(4*H*)-yl)-benzoate (9). Yield: 8.3 mg, ^{1}H NMR (400 MHz, DMSO-d_6) δ 8.21 (d, 2H, J = 8.5 Hz, Ar), 7.95 (d, 1H, J = 8.0 Hz, Ar), 7.63 (d, 2H, J = 8.5 Hz, Ar), 7.55 (dd, 1H, J = 8.0, 8.0 Hz, Ar), 7.41−7.33 (m, 1H, Ar), 4.35 (q, 2H, J = 7.0 Hz, CH_2), 3.33 (br s, 4H, CH), 2.87 (br s, 4H, CH), 2.67 (s, 3H, NMe), 1.35 (t, 3H, J = 7.0 Hz, CH_3; MS (ESI) m/z 412 [$(M + H)^+$], RT, 0.93 min; purity, 100% (ELSD), 95% (PDA).

Synthesis of 3-(4-Methoxyphenyl)-2-(4-methylpiperazin-1-yl)-quinazolin-4(3*H*)-one (10). (Step A) 2-Amino-*N*-(4-methoxyphenyl)-benzamide (**47e**)

p-Anisidine **46b** (830 mg, 6.74 mmol, 1.1 equiv) was added to a solution of isatoic anhydride **45d** (1.0 g, 6.13 mmol, 1.0 equiv) in toluene (6.1 mL) and stirred at reflux for 4 h. After diluting with hexane (10 mL), the reaction mixture was filtered out to collect the precipitate. The precipitate was dried in reduced pressure to give amide **47e** (1.43 g, 96%) as a gray solid, with MS (ESI) m/z 243 [$(M + H)^+$], RT 1.32 min.

(Step B) 3-(4-Methoxyphenyl)-2-thioxo-2,3-dihydroquinazolin-4(1*H*)-one (**48e**)

A solution of amide **47e** (500 mg, 2.06 mmol, 1.0 equiv) in EtOH (4 mL) was added to a solution of NaOH (124 mg, 3.10 mmol, 1.5 equiv) in CS_2 (187 μL, 3.10 mmol, 1.5 equiv), and the reaction mixture was stirred at reflux for 16 h. After cooling to rt, the reaction mixture was poured to 1 M $HCl_{(aq)}$ (10 mL) and diluted with hexane (10 mL). The suspension was filtered to collect the precipitate, and the solid was dried to give the cyclic compound **48e** (679 mg, quant) as a white solid, with MS (ESI) m/z 285 [$(M + H)^+$], RT 1.30 min.

(Step C) 2-Chloro-3-(4-methoxyphenyl)-quinazolin-4(3*H*)-one (**49e**)

Sulfuryl chloride (58 μL, 0.704 mmol, 1.0 equiv) was added to a solution of thiocarbonyl compound **48e** (200 mg, 0.704 mmol, 1.0 equiv) in $CHCl_3$ (1.4 mL) and stirred at reflux for 1 h. After cooling to rt, the reaction mixture was quenched with H_2O (10 mL) and extracted with $CHCl_3$ (20 mL × 3). The organic layer was combined, dried over $MgSO_4$, and evaporated with reduced pressure to give chloride **49e** (139 mg, 69%) as a colorless solid, with MS (ESI) m/z 287 [$(M + H)^+$], RT, 1.56 min.

(Step D) 3-(4-Methoxyphenyl)-2-(4-methylpiperazin-1-yl)-quinazolin-4(3*H*)-one (**10**)

1-Methylpiperazine **43a** was added to a solution of chloride **49e** (40 mg, 0.14 mmol, 1.0 equiv) in DMSO (500 μL) and stirred at 125 °C for 1 h. The reaction mixture directly purified with column chromatography on silica with 90:10 $CHCl_3$/MeOH as eluent gave **10** (16.6 mg, 34%) as a colorless solid, ^{1}H NMR (400 MHz, DMSO-d_6) δ 8.11 (d, 1H, J = 7.5 Hz, Ar), 7.75 (dd, 1H, J = 7.5, 7.5 Hz, Ar), 7.57 (d, 1H, J = 7.5 Hz, Ar), 7.39−7.33 (m, 3H, Ar), 7.09 (d, 1H, J = 7.5 Hz, Ar), 3.23 (br t, 4H, J = 5.0 Hz, CH), 2.24 (br t, 4H, J = 5.0 Hz, CH), 2.22 (s, 3H, NMe); ^{13}C NMR (100.6 MHz, DMSO-d_6) δ 164.05 (C═O), 154.48 (*ipso*-Ar), 154.48 (*ipso*-Ar), 147.89 (*ipso*-Ar), 134.57 (Ar), 129.74 (Ar), 129.62 (*ipso*-Ar), 126.53 (Ar), 125.66 (Ar), 124.58 (Ar), 118.80 (*ipso*-Ar), 113.77 (Ar), 54.63 (OMe), 53.70 (CH_2), 47.84 (CH_2), 44.53 (CH_3); MS (ESI) m/z 352 [$(M + 2H)^+$], rt, 0.76 min; purity, 100% (ELSD), 100% (PDA).

Ethyl 4-(8-Bromo-2-(4-methylpiperazin-1-yl)-4-oxoquinazolin-3(4*H*)-yl)-benzoate (11). Yield: 6.2 mg, ^{1}H NMR (400 MHz, DMSO-d_6) δ 8.07 (d, 2H, J = 8.5 Hz, Ar), 7.95 (dd, 1H, J = 8.0, 1.5 Hz, Ar), 7.87 (dd, 1H, J = 8.0, 1.5 Hz, Ar), 7.64 (d, 2H, J = 8.5 Hz, Ar), 7.27 (dd, 1H, J = 8.0, 8.0 Hz, Ar), 4.35 (q, 2H, J = 7.0 Hz, CH_2), 3.14−3.10 (m, 4H, CH), 2.54 (s, 3H, NMe), 2.16−2.13 (m, 4H, CH), 1.35 (t, 3H, J = 7.0 Hz, CH_3); MS (ESI) m/z 473 [$(M + H)^+$], RT, 1.07 min; purity, 100% (ELSD), 97% (PDA).

Ethyl 4-(8-Methoxy-2-(4-methylpiperazin-1-yl)-4-oxoquinazolin-3(4*H*)-yl)-benzoate (12). Yield: 5.4 mg, ^{1}H NMR (400 MHz, DMSO-d_6) δ 8.08 (d, 2H, J = 8.5 Hz, Ar), 7.63 (d, 2H, J = 8.5 Hz, Ar), 7.59 (dd, 1H, J = 8.0, 1.5 Hz, Ar), 7.33 (dd, 1H, J = 8.0, 1.5 Hz, Ar), 7.29 (dd, 1H, J = 8.0, 8.0 Hz, Ar), 4.36 (q, 2H, J = 7.0 Hz, CH_2), 3.92 (s, 3H, OMe), 3.26−3.23 (m, 4H, CH), 3.04−2.99 (m, 4H, CH), 2.54 (s, 3H, NMe), 1.36 (t, 3H, J = 7.0 Hz, CH_3); MS (ESI) m/z 366 [$(M + H)^+$], rt, 0.80 min; purity, 100% (ELSD), 98% (PDA).

Ethyl 4-(8-Fluoro-2-(4-isopropylpiperazin-1-yl)-4-oxoquinazolin-3(4*H*)-yl)-benzoate (13). Yield: 3.0 mg, ^{1}H NMR (400 MHz, DMSO-d_6) δ 8.08 (d, 2H, J = 8.5 Hz, Ar), 7.82 (d, 1H, J = 8.0 Hz, Ar), 7.64 (d, 2H, J = 8.5 Hz, Ar), 7.62−7.59 (m, 1H, Ar), 7.34−7.27 (m, 1H, Ar), 4.35 (q, 2H, J = 7.0 Hz, CH_2), 3.07−3.04 (m, 4H, CH), 2.54 (s, 3H, NMe), 2.16−2.13 (m, 4H, CH), 1.35 (t, 3H, J = 7.0 Hz, CH_3), 1.31−1.23 (m, 1H, CH), 0,85 (d, 6H, J = 7.0 Hz, CH); MS (ESI) m/z 440 [$(M + H)^+$], RT, 1.00 min; purity, 98% (ELSD), 95% (PDA).

Ethyl 4-(2-(3-(Dimethylamino)-pyrrolidin-1-yl)-8-fluoro-4-oxoquinazolin-3(4*H*)-yl)-benzoate (14). Yield: 4.7 mg, ^{1}H NMR (400 MHz, DMSO-d_6) δ 8.14−8.05 (m, 2H, Ar), 7.75 (d, 1H, J = 8.0 Hz, Ar), 7.58−7.50 (m, 3H, Ar), 7.19−7.13 (m, 1H, Ar), 4.36 (q, 2H, J

DOI: 10.1021/acs.jmedchem.8b01615
J. Med. Chem. 2019, 62, 1468−1483

= 7.0 Hz, CH_2), 3.31−3.27 (m, 4H, CH), 3.07−2.98 (m, 1H, CH), 2.00 (s, 6H, NMe), 1,92−1,83 (m, 1H, CH), 1.55−1.42 (m, 1H, CH), 1.35 (t, 3H, J = 7.0 Hz, CH_3); MS (ESI) m/z 426 [$(M + H)^+$], RT, 0.97 min; purity, 98% (ELSD), 95% (PDA).

Ethyl 4-(8-Fluoro-2-(methyl(1-methylpyrrolidin-3-yl)-amino)-4-oxoquinazolin-3(4*H*)-yl)-benzoate (15). Yield: 7.8 mg, ^{1}H NMR (400 MHz, DMSO-d_6) δ 8.14 (d, 2H, J = 8.0 Hz, Ar), 7.79 (d, 2H, J = 8.0, Ar), 7.71 (d, 1H, J = 8.0 Hz, Ar), 7.52−7.48 (m, 1H, Ar), 7.28−7.23 (m, 1H, Ar), 4.36 (q, 2H, J = 7.0 Hz, CH_2), 3.00 (s, 3H, NMe), 2.82 (d, 1H, J = 1.0 Hz, CH), 2.77 (d, 2H, J = 4.5 Hz, CH), 2.71−2.65 (m, 2H, CH), 2.62 (s, 3H, NMe), 2.17 (m, 2H, CH), 1.35 (t, 3H, J = 7.0 Hz, CH_3); MS (ESI) m/z 426 [$(M + H)^+$], RT, 0.91 min; purity, 100% (ELSD), 96% (PDA).

Synthesis of 7-Fluoro-3-(4-methoxyphenyl)-2-(piperazin-1-yl)- quinazolin-4(3*H*)-one (16). (Step A) *tert*-Butyl 4-(7-fluoro-3-(4-methoxyphenyl)-4-oxo-3,4-dihydroquinazolin -2-yl)-piperazine-1-carboxylate (**51a**)

tert-Butyl 1-piperazine carboxylate **50b** (24.6 mg, 131 μmol, 2.0 equiv) was added to a solution of chloride **49d** (20 mg, 66 μmol, 1.0 equiv) in DMSO (500 μL) and stirred at 125 °C for 1 h. The reaction mixture directly purified with column chromatography on silica with 90:10 $CHCl_3$/MeOH as eluent gave **51a** (37.7 mg, quant) as a colorless solid, with MS (ESI) m/z 455 [$(M + H)^+$], RT, 1.93 min.

(Step B) 7-Fluoro-3-(4-methoxyphenyl)-2-(piperazin-1-yl)-quinazolin-4(3*H*)-one (**16**)

TFA (95 mg, 0.83 mmol, 10 equiv) was added to a solution of chloride **51a** (37.7 mg, 83 μmol, 1.0 equiv) in CH_2Cl_2 (830 μL) and stirred at RT for 1 h. The reaction mixture was neutralized with $NH_4OH_{(aq)}$ and evaporated to give the crude product. Purification with column chromatography on silica with 90:10 $CHCl_3$/MeOH as eluent gave **16** (37.7 mg, quant) as a colorless solid, ^{1}H NMR (400 MHz, DMSO-d_6) δ 8.19 (dd, 1H, J = 8.0, 6.0 Hz, Ar), 7.39 (d, 2H, J = 8.0 Hz, Ar), 7.25 (dd, 1H, J = 10.0, 3.0 Hz, Ar), 7.19 (ddd, 1H, J = 8.0, 8.0, 2.5 Hz, Ar), 7.12 (d, 2H, J = 8.0, Hz, Ar), 3.43 (br t, 4H, J = 5.0 Hz, CH), 3.04 (br t, 4H, J = 5.0 Hz, CH); MS (ESI) m/z 355 [$(M + H)^+$], RT, 0.86 min; purity, 100% (ELSD), 100% (PDA).

Synthesis of 7-Fluoro-3-(4-methoxyphenyl)-2-(4-methylpiperazin-1-yl)-quinazolin-4(3*H*)-one (17). (Step A) 2-Amino-4-fluoro-*N*-(4-methoxyphenyl)-benzamide (**47d**) was prepared from **45c** analogous to the synthesis of **47e** from **45d** to afford **47d** (650 mg, 90%) as a gray solid, with MS (ESI) m/z 261 [$(M + H)^+$], RT, 1.41 min.

(Step B) 7-Fluoro-3-(4-methoxyphenyl)-2-thioxo-2,3-dihydroquinazolin-4(1*H*)-one (**48d**) was prepared from **47d** analogous to the synthesis of **48e** from **47e** to afford **48d** (251 mg, quant) as a colorless solid, with MS (ESI) m/z 303 [$(M + H)^+$], RT, 1.38 min.

(Step C) 2-Chloro-7-fluoro-3-(4-methoxyphenyl)-quinazolin-4(3*H*)-one (**49d**) was prepared from **48d** analogous to the synthesis of **49e** from **48e** to afford **49d** (66.4 mg, 66%) as a colorless solid, MS (ESI) m/z 305 [$(M + H)^+$], RT, 4.34 min (condition B).

(Step D) 7-Fluoro-3-(4-methoxyphenyl)-2-(4-methylpiperazin-1-yl)-quinazolin-4(3*H*)-one (**17**) was prepared from **49d** analogous to the synthesis of **10** from **49e** to afford **17** (23.2 mg, 95%) as a colorless solid, ^{1}H NMR (400 MHz, DMSO-d_6) δ 8.14 (dd, 1H, J = 8.0, 6.0 Hz, Ar), 7.34 (d, 2H, J = 8.0 Hz, Ar), 7.21 (dd, 1H, J = 10.0, 3.0 Hz, Ar), 7.12 (ddd, 1H, J = 8.0, 8.0, 2.5 Hz, Ar), 7.09 (d, 2H, J = 8.0, Hz, Ar), 3.23 (br t, 4H, J = 5.0 Hz, CH), 2.24 (br t, 4H, J = 5.0 Hz, CH), 2.22 (s, 3H, NMe); MS (ESI) m/z 423 [$(M + H)^+$], RT 1.11 min.

2-(4-Ethylpiperazin-1-yl)-7-fluoro-3-(4-methoxyphenyl)-quinazolin-4(3*H*)-one (18). **18** was prepared from **49d** with 1-ethylpiperazine **50a** analogous to the synthesis of **10** from **49e** to afford **18** (22.1 mg, 88%) as a colorless solid, ^{1}H NMR (400 MHz, DMSO-d_6) δ 8.14 (dd, 1H, J = 8.0, 6.0 Hz, Ar), 7.34 (d, 2H, J = 8.0 Hz, Ar), 7.21 (dd, 1H, J = 10.0, 3.0 Hz, Ar), 7.14−7.05 (m, 3H, Ar), 3.24 (br t, 4H, J = 5.0 Hz, CH), 2.36 (q, 2H, J = 7.0 Hz, CH_2), 2.26 (br t, 4H, J = 5.0 Hz, CH), 1.06 (t, 3H, J = 7.0 Hz, CH); MS (ESI) m/z 423 [$(M + H)^+$], RT, 1.11 min; purity, 100% (ELSD), 100% (PDA).

2-((2-(Dimethylamino)-ethyl)amino)-3-(4-methoxyphenyl)-quinazolin-4(3*H*)-one (19). *N*,*N*′-Dimethylethylenediamine **43e** (19 μL, 0.21 mmol, 2.0 equiv) was added to a solution of chloride (40 mg, 0.14 mmol, 1.0 equiv) in DMSO (500 μL) and stirred at 125 °C for 1 h. The reaction mixture directly purified with column chromatography on silica with 90:10 $CHCl_3$/MeOH as eluent gave **19** (5.5 mg, 16%) as a yellow oil, ^{1}H NMR (400 MHz, DMSO-d_6) δ 8.02 (d, 1H, J = 8.0 Hz, Ar), 7.66 (dd, 1H, J = 8.0, 8.0 Hz, Ar), 7.41 (d, 1H, J = 8.0 Hz, Ar), 7.29−7.25 (m, 2H, Ar), 7.23−7.12 (m, 3H, Ar), 3.57 (br t, 4H, J = 5.0 Hz, CH), 2.68 (br t, 4H, J = 5.0 Hz, CH), 2.39 (s, 6H, NMe); ^{13}C NMR (100.6 MHz, DMSO-d_6) δ 163.53 (C═O), 160.71 (*ipso*-Ar), 149.56 (*ipso*-Ar), 134.53 (Ar), 129.74 (Ar), 126.81 (*ipso*-Ar), 126.41 (Ar), 124.28 (Ar), 122.15 (Ar), 116.96 (*ipso*-Ar), 115.27 (Ar), 57.72 (CH_3), 54.68 (CH_2), 43.76 (CH_3), 38.36 (CH_2); MS (ESI) m/z 423 [$(M + H)^+$], RT, 1.11 min; purity, 100% (ELSD), 100% (PDA).

Synthesis of (*S*)-7-Fluoro-2-(3-isopropyl-4-methylpiperazin-1-yl)-3-(4-(trifluoromethoxy)-phenyl)-quinazolin-4(3*H*)-one (20). (Step A) *tert*-Butyl (*S*)-4-(7-fluoro-4-oxo-3-(4-(trifluoromethoxy)-phenyl)-3,4-dihydro-quinazolin-2-yl)-2-isopropylpiperazine-1-carboxylate was prepared from **49c** with (*S*)-*N*-Boc-2-isopropylpiperazine **50c** analogous to the synthesis of **51a** from **49d** to afford **51b** (20.8 mg, 46%) as a colorless solid, MS (ESI) m/z 551 [$(M + H)^+$], RT, 2.29 min.

(Step B) (*S*)-7-Fluoro-2-(3-isopropyl-4-methylpiperazin-1-yl)-3-(4-(trifluoromethoxy) -phenyl)-quinazolin-4(3*H*)-one (**20**)

$HCl_{(aq)}$ (35%, 200 μL) was added to a solution of **51b** (20.8 mg, 38 μmol, 1.0 equiv) in MeOH (300 μL) and stirred at RT for 1 h. After evaporating the solvent, the residue was dissolved to 1,2-dichloroethane/AcOH (3:1) (420 μL) and then 35% $HCHO_{(aq)}$ (160 mL) was added to the reaction mixture at rt. After stirring for 10 min at rt, $NaBH(OAc)_3$ (24 mg) was added to the reaction mixture at 0 °C, then stirred for 16h at rt. The reaction mixture directly purified with column chromatography on silica with 100:9:1 $CHCl_3$/MeOH/NH_4OH as eluent gave **20** (12.7 mg, 72%) as a colorless solid, ^{1}H NMR (400 MHz, DMSO-d_6) δ 8.16 (dd, 1H, J = 8.0, 6.0 Hz, Ar), 7.60 (br s, 2H, Ar), 7.47 (d, 2H, J = 8.0 Hz, Ar), 7.24 (dd, 1H, J = 10.0, 3.0 Hz, Ar), 7.13 (ddd, 1H, J = 10.0, 10.0, 3.0 Hz, Ar), 3.52 (dd, 1H, J = 12.0, 3.0 Hz, CH), 3.36−3.32 (1H, m, CH), 3.04 (ddd, 1H, J = 12.0, 12.0, 3.0 Hz, CH), 2.77 (ddd, 1H, J = 12.0, 3.0, 3.0 Hz, CH), 2.52 (dd, 1H, J = 12.0, 12.0 Hz, CH), 2.18 (s, 3H, NMe), 2.12 (ddd, 1H, J = 12.0, 12.0, 3.0 Hz, CH), 2.05−1.93 (m, 1H, CH), 1.45 (ddd, 1H, J = 12.0, 3.0, 3.0 Hz, CH), 0.80 (d, 1H, J = 7.5 Hz, CH_3), 0.66 (d, 1H, J = 7.5 Hz, CH_3); ^{13}C NMR (100.6 MHz, DMSO-d_6) δ 162.64 (C═O), 155.12 (*ipso*-Ar), 148.58 (*ipso*-Ar), 135.87 (Ar), 134.67 (Ar), 130.26 (Ar), 129.67 (Ar), 121.28 (Ar), 113.12 (Ar), 110.62 (*ipso*-Ar), 66.68 (CH), 55.14 (CH_2), 40.85 (CH_3), 26.17 (CH_2), 18.76 (CH_2), 14.00 (CH_2); MS (ESI) m/z 466 [$(M + H)^+$], RT, 1.27 min; purity, 100% (ELSD), 100% (PDA).

Synthesis of (*S*)-7-Fluoro-2-(3-isobutyl-4-methylpiperazin-1-yl)-3-(4-(trifluoromethoxy)-phenyl)-quinazolin-4(3*H*)-one (21). (Step A) *tert*-butyl (*S*)-4-(7-fluoro-4-oxo-3-(4-(trifluoromethoxy)-phenyl)-3,4-dihydro -quinazolin-2-yl)-2-isobutylpiperazine-1-carboxylate was prepared from **49c** with (*S*)-*N*-Boc-2-isobutylpiperazine **50d** analogous to the synthesis of **51a** from **49d** to afford **51c** (18.4 mg, 39%) as a colorless solid, with MS (ESI) m/z 565 [$(M + H)^+$], RT, 2.38 min.

(Step B) (*S*)-7-Fluoro-2-(3-isobutyl-4-methylpiperazin-1-yl)-3-(4-(trifluoromethoxy)-phenyl)-quinazolin-4(3*H*)-one (**21**) was prepared from **51c** analogous to the synthesis of **51b** from **20** to afford **21** (15.9 mg, quant) as a colorless solid, ^{1}H NMR (400 MHz, DMSO-d_6) δ 8.16 (dd, 1H, J = 8.0, 6.0 Hz, Ar), 7.60 (br s, 2H, Ar), 7.47 (d, 2H, J = 8.0 Hz, Ar), 7.24 (dd, 1H, J = 10.0, 3.0 Hz, Ar), 7.14 (ddd, 1H, J = 10.0, 10.0, 3.0 Hz, Ar), 3.48 (dd, 1H, J = 12.0, 3.0 Hz, CH), 3.04 (ddd, 1H, J = 12.0, 12.0, 3.0 Hz, CH), 2.73 (ddd, 1H, J = 12.0, 3.0, 3.0 Hz, CH), 2.50 (dd, 1H, J = 12.0, 12.0 Hz, CH), 2.23 (s, 3H, NMe), 2.13 (ddd, 1H, J = 12.0, 12.0, 3.0 Hz, CH), 1.45−1.27 (m, 2H, CH), 1.00 (ddd, 1H, J = 12.0, 10.0, 3.0 Hz, CH), 0.88 (d, 1H, J = 7.5 Hz, CH_3), 0.78 (d, 1H, J = 7.5 Hz, CH_3); ^{13}C NMR (100.6 MHz, DMSO-d_6) δ 162.64 (C═O), 154.67 (*ipso*-Ar), 150.11 (*ipso*-Ar), 148.66 (*ipso*-Ar), 135.72 (Ar), 129.68 (Ar), 129.57 (Ar), 121.05 (Ar), 115.59 (*ipso*-Ar), 113.20 (Ar), 112.96 (Ar), 110.88 (Ar), 110.67 (Ar), 60.05 (CH), 54.19 (CH_2), 52.95 (CH_2), 41.02 (CH_3), 38.86 (CH_2), 24.96 (CH_2), 22.85 (CH_3), 20.97 (CH_3); MS (ESI) m/z 480 [$(M + H)^+$], RT, 1.38 min; purity, 100% (ELSD), 100% (PDA).

DOI: 10.1021/acs.jmedchem.8b01615
J. Med. Chem. 2019, 62, 1468−1483

Synthesis of 7-Fluoro-3-(4-(trifluoromethoxy)-phenyl)-2-(3,3,4-trimethylpiperazin-1-yl)-quinazolin-4(3*H*)-one (22). (Step A) *tert*-Butyl 4-(7-fluoro-4-oxo-3-(4-(trifluoromethoxy)-phenyl)-3,4-dihydro-quinazolin-2-yl)-2,2-dimethylpiperazine-1-carboxylate was prepared from **49c** with 1-Boc-2,2-dimethyl-piperazine **50e** analogous to the synthesis of **51a** from **49d** to afford **51d** (19.2 mg, 43%) as a colorless solid, with MS (ESI) *m*/*z* 537 [(M + H)$^+$], RT, 2.24 min.

(Step B) 7-Fluoro-3-(4-(trifluoromethoxy)-phenyl)-2-(3,3,4-trimethylpiperazin-1-yl)-quinazolin-4(3*H*)-one (**22**) was prepared from **51d** analogous to the synthesis of **51b** from **20** to afford **22** (14.8 mg, 92%) as a colorless solid, ^{1}H NMR (400 MHz, DMSO-d_6) δ 8.17 (dd, 1H, *J* = 8.0, 6.0 Hz, Ar), 7.62−7.56 (m, 2H, Ar), 7.50 (d, 2H, *J* = 8.0 Hz, Ar), 7.27 (dd, 1H, *J* = 10.0, 3.0 Hz, Ar), 7.17 (ddd, 1H, *J* = 10.0, 10.0, 3.0 Hz, Ar), 3.23 (dd, 2H, *J* = 12.0, 3.0 Hz, CH), 3.00 (br s, 2H, CH), 2.48 (dd, 1H, *J* = 6.5, 6.5 Hz, CH), 2.50 (dd, 1H, *J* = 6.5, 6.5 Hz, CH), 2.28 (s, 3H, NMe), 1.97 (s, 2H, CH), 0.88 (s, 6H, CH_3); ^{13}C NMR (100.6 MHz, DMSO-d_6) δ 162.75 (C═O), 155.25 (*ipso*-Ar), 150.11 (*ipso*-Ar), 150.06 (*ipso*-Ar), 135.85 (Ar), 131.10 (Ar), 129.66 (Ar), 129.55 (Ar), 121.44 (Ar), 115.85 (*ipso*-Ar), 113.57 (Ar), 113.33 (Ar), 111.13 (Ar), 110.91 (Ar), 59.59 (C), 54.95 (CH_2), 48.72 (CH_2), 48.53 (CH_2), 35.66 (CH_3); MS (ESI) *m*/*z* 452 [(M + H)$^+$], RT, 1.20 min; purity, 100% (ELSD), 100% (PDA).

Synthesis of 7-Fluoro-2-(4-methyl-4,7-diazaspiro[2.5]octan-7-yl)-3-(4-(trifluoromethoxy)-phenyl)-quinazolin-4(3*H*)-one (23). (Step A) *tert*-Butyl 7-(7-fluoro-4-oxo-3-(4-(trifluoromethoxy)-phenyl)-3,4-dihydro-quinazolin-2-yl)-4,7-diazaspiro[2.5]octane-4-carboxylate was prepared from **49c** with 4,7-Diaza-spiro[2,5]octane-4-carboxylic acid *tert*-butyl ester **50f** analogous to the synthesis of **51a** from **49d** to afford **51e** (18.8 mg, 42%) as a colorless solid, with MS (ESI) *m*/*z* 535 [(M + H)$^+$], RT 2.22 min.

(Step B) 7-Fluoro-2-(4-methyl-4,7-diazaspiro[2.5]octan-7-yl)-3-(4-(trifluoromethoxy)-phenyl)-quinazolin-4(3*H*)-one (**23**) was prepared from **51f** analogous to the synthesis of **51b** from **20** to afford **23** (10.7 mg, 68%) as a colorless solid, ^{1}H NMR (400 MHz, DMSO-d_6) δ 8.16 (dd, 1H, *J* = 8.0, 6.0 Hz, Ar), 7.61−7.56 (m, 2H, Ar), 7.48 (d, 2H, *J* = 8.0 Hz, Ar), 7.24 (dd, 1H, *J* = 10.0, 3.0 Hz, Ar), 7.14 (ddd, 1H, *J* = 10.0, 10.0, 3.0 Hz, Ar), 3.26−3.22 (m, 2H, CH), 3.02 (br s, 2H, CH), 2.69−2.65 (m, 1H, CH), 2.34 (s, 3H, NMe), 0.56 (dd, 2H, *J* = 5.5, 5.5 Hz, CH_2), 0.11 (dd, 2H, *J* = 5.5, 5.5 Hz, CH_2); ^{13}C NMR (100.6 MHz, DMSO-d_6) δ 162.75 (C═O), 155.34 (*ipso*-Ar), 150.33 (*ipso*-Ar), 148.53 (*ipso*-Ar), 136.04 (Ar), 130.92 (Ar), 129.66 (Ar), 129.55 (Ar), 121.23 (Ar), 115.72 (*ipso*-Ar), 113.19 (Ar), 112.95 (Ar), 110.88 (Ar), 110.65 (Ar), 50.45 (CH_2), 50.23 (CH_2), 42.65 (CH_2), 40.60 (CH_3), 35.57 (CH_2), 10.09 (CH_2); MS (ESI) *m*/*z* 450 [(M + H)$^+$], RT, 1.20 min; purity, 100% (ELSD), 100% (PDA).

Synthesis of (*R*)-2-(2,4-Dimethylpiperazin-1-yl)-7-fluoro-3-(4-(trifluoromethoxy)-phenyl)-quinazolin-4(3*H*)-one (24). (Step A) *tert*-Butyl (*R*)-4-(7-fluoro-4-oxo-3-(4-(trifluoromethoxy)-phenyl)-3,4-dihydro quinazolin-2-yl)-3-methylpiperazine-1-carboxylate was prepared from **49c** with (*R*)-*N*-Boc-3-methylpiperazine **50g** analogous to the synthesis of **51a** from **49d** to afford **51f** (10.4 mg, 24%) as a colorless solid, with MS (ESI) *m*/*z* 523 [(M + H)$^+$], RT, 2.18 min.

(Step B) (*R*)-2-(2,4-Dimethylpiperazin-1-yl)-7-fluoro-3-(4-(trifluoromethoxy)-phenyl)-quinazolin-4(3*H*)-one (**24**) was prepared from **51f** analogous to the synthesis of **51b** from **20** to afford **24** (4.9 mg, 57%) as a colorless solid, ^{1}H NMR (400 MHz, DMSO-d_6) δ 8.18 (dd, 1H, *J* = 8.0, 6.0 Hz, Ar), 8.13 (dd, 1H, *J* = 8.0, 6.0 Hz, Ar), 7.56−7.43 (m, 4H, Ar), 7.26 (dd, 1H, *J* = 10.0, 2.5 Hz, Ar), 7.17 (ddd, 1H, *J* = 10.0, 10.0, 2.5 Hz, Ar), 7.05 (ddd, 1H, *J* = 10.0, 10.0, 2.5 Hz, Ar), 6.97 (dd, 1H, *J* = 10.0, 2.5 Hz, Ar), 3.68−3.61 (m, 2H, CH), 3.23−3.19 (m, 2H, CH), 2.30−2.22 (m, 2H, CH), 2.18 (s, 3H, NMe), 2.18−2.14 (m, 1H, CH), 1.13 (d, 3H, *J* = 6.5 Hz, CH_3); ^{13}C NMR (100.6 MHz, DMSO-d_6) δ 162.52 (C═O), 154.62 (*ipso*-Ar), 143.57 (*ipso*-Ar), 135.82 (*ipso*-Ar), 134.67 (Ar), 133.87 (*ipso*-Ar), 130.57 (Ar), 121.36 (Ar) 115.40 (*ipso*-Ar), 113.53 (Ar), 113.29 (Ar), 111.19 (Ar), 110.73 (Ar), 59.6 (CH), 53.78 (CH_2), 51.53 (CH_2), 44.79 (CH_3), 14.43 (CH_3); MS (ESI) *m*/*z* 437 [(M + H)$^+$], RT, 1.23 min; purity, 100% (ELSD), 100% (PDA).

7-Fluoro-2-(4-methyl-3-oxopiperazin-1-yl)-3-(4-(trifluoromethoxy)-phenyl)-quinazolin-4(3*H*)-one (25). **25** was prepared from **49c** with 1-methylpiperazin-2-one **50h** analogous to the synthesis of **51a** from **49d** to afford **25** (23.3 mg, 53%) as a colorless solid, ^{1}H NMR (400 MHz, DMSO-d_6) δ 8.16 (dd, 1H, *J* = 8.0, 6.0 Hz, Ar), 7.61−7.56 (m, 2H, Ar), 7.49 (d, 2H, *J* = 8.0 Hz, Ar), 7.25 (dd, 1H, *J* = 10.0, 3.0 Hz, Ar), 7.15 (ddd, 1H, *J* = 10.0, 10.0, 3.0 Hz, Ar), 3.84 (br s, 2H, CH), 3.37 (dd, 2H, *J* = 5.0, 5.0 Hz, CH), 3.06 (dd, 2H, *J* = 5.0, 5.0 Hz, CH), 2.89 (s, 3H, NMe); ^{13}C NMR (100.6 MHz, DMSO-d_6) δ 166.81 (C═O), 162.57 (C═O), 153.16 (*ipso*-Ar), 150,02 (*ipso*-Ar), 149.89 (*ipso*-Ar), 148.78 (Ar), 135.57 (Ar), 130.70 (Ar), 129.67 (Ar), 129.56 (Ar), 121.40 (Ar), 115.70 (*ipso*-Ar), 113.39 (Ar), 113.16 (Ar), 111.07 (Ar), 110.86 (Ar), 51.15 (CH_2), 45.59 (CH_2), 32.90 (CH_3); MS (ESI) *m*/*z* 438 [(M + H)$^+$], RT, 1.53 min; purity, 100% (ELSD), 100% (PDA).

8-Fluoro-2-(4-methylpiperazin-1-yl)-3-(4-(trifluoromethyl)-phenyl)-quinazolin-4(3*H*)-one (26). Yield: 4.5 mg, ^{1}H NMR (400 MHz, DMSO-d_6) δ 7.92 (d, 2H, *J* = 8.5 Hz, Ar), 7.83 (d, 1H, *J* = 8.0 Hz, Ar), 7.76 (d, 2H, *J* = 8.5 Hz, Ar), 7.67−7.61 (m, 1H, Ar), 7.36−7.30 (m, 1H, Ar), 3.05 (dd, 4H, *J* = 4.5, 4.5 Hz, CH), 2.06−2.00 (m, 4H, CH), 2.05 (s, 3H, NMe); MS (ESI) *m*/*z* 408 [(M + H)$^+$], RT, 0.97 min; purity, 96% (ELSD), 96% (PDA).

8-Fluoro-3-(4-isopropylphenyl)-2-(4-methylpiperazin-1-yl)-quinazolin-4(3*H*)-one (27). Yield: 4.1 mg, ^{1}H NMR (400 MHz, DMSO-d_6) δ 7.95 (d, 1H, *J* = 8.0 Hz, Ar), 7.55 (dd, 1H, *J* = 9.0 Hz, Ar), 7.48 (d, 2H, *J* = 8.0 Hz, Ar), 7.40 (d, 2H, *J* = 8.0 Hz, Ar), 7.40−7.35 (m, 1H, Ar), 3.81 (br s, 4H, CH), 3.08−3.01 (m, 4H, CH), 2.86 (s, 3H, NMe); MS (ESI) *m*/*z* 382 [(M + H)$^+$], RT, 1.00 min; purity, 97% (ELSD), 96% (PDA).

8-Fluoro-2-(4-methylpiperazin-1-yl)-3-(4-(trifluoromethoxy)-phenyl)-quinazolin-4(3*H*)-one (28). Yield: 4.8 mg, ^{1}H NMR (400 MHz, DMSO-d_6) δ 7.92 (d, 1H, *J* = 8.0 Hz, Ar), 7.63−7.58 (m, 2H, Ar), 7.55−7.46 (m, 3H, Ar), 7.33 (ddd, 1H, *J* = 8.0, 8.0, 5.0 Hz, Ar), 3.23 (br t, 4H, *J* = 5.0 Hz, CH), 2.23 (br t, 4H, *J* = 5.0 Hz, CH), 2.24 (s, 3H, NMe); ^{13}C NMR (100.6 MHz, DMSO-d_6) δ 162.59 (C═O), 157.57 (*ipso*-Ar), 155.06 (*ipso*-Ar), 154.12 (*ipso*-Ar), 148.60 (*ipso*-Ar), 137.29 (*ipso*-Ar), 137.17 (*ipso*-Ar), 135.90 (Ar), 130.74 (Ar), 124.49 (Ar), 124.42 (Ar), 122.13 (Ar), 122.10 (Ar), 121.19 (Ar), 121.76−129.90−119.88−119.22 (CF_3), 119.69 (*ipso*-Ar), 53.46 (CH_2), 48.15 (CH_2), 44.48 (CH_3); MS (ESI) *m*/*z* 424 [(M + H)$^+$], RT, 1.01 min; purity, 100% (ELSD), 100% (PDA).

8-Fluoro-2-(4-methylpiperazin-1-yl)-3-(4-((trifluoromethyl)-thio)-phenyl)-quinazolin-4(3*H*)-one (29). Yield: 4.0 mg, ^{1}H NMR (400 MHz, DMSO-d_6) δ 7.95 (d, 1H, *J* = 8.0 Hz, Ar), 7.92 (d, 2H, *J* = 8.0 Hz, Ar), 7.69−7.64 (m, 2H, Ar), 7.59−7.52 (m, 2H, Ar), 7.39 (ddd, 1H, *J* = 8.0, 8.0, 5.0 Hz, Ar), 3.39 (br s, 4H, CH), 2.92 (br s, 4H, CH), 2.71 (s, 3H, NMe); ^{13}C NMR (100.6 MHz, DMSO-d_6) δ 162.12 (C═O), 162.08 (*ipso*-Ar), 157.62 (*ipso*-Ar), 155.13 (*ipso*-Ar), 152.51 (*ipso*-Ar), 148.60 (*ipso*-Ar), 139.31 (*ipso*-Ar), 136.77 (Ar), 136.66 (Ar), 130.08 (Ar), 125.36 (Ar), 125.29 (Ar), 124.71 (Ar), 122.30 (Ar), 121.10 (Ar), 121.27 (CF_3), 120.16 (*ipso*-Ar), 119.97 (*ipso*-Ar), 52.19 (CH_2), 45.83 (CH_2), 42.22 (CH_3); MS (ESI) *m*/*z* 440 [(M + H)$^+$], RT, 1.08 min; purity, 100% (ELSD), 95% (PDA).

8-Fluoro-2-(4-methylpiperazin-1-yl)-3-(4-((trifluoromethyl)-thio)-phenyl)-quinazolin-4(3*H*)-one HCl Salt (29·HCl). HCl (1 M) in MeOH (23 μL, 23 μmol, 1.0 equiv) was added to a stirred solution of **29** (10 mg, 23 μmol, 1.0 equiv) in MeOH (0.5 mL) at RT and stirred at the same temperature for 10 min. Then, the solvent was removed in vacuo to give **29·HCl** (10.8 mg, 99%) as a colorless solid, ^{1}H NMR (400 MHz, DMSO-d_6) δ 7.91 (d, 1H, *J* = 8.0 Hz, Ar), 7.86 (d, 2H, *J* = 8.0 Hz, Ar), 7.73−7.67 (m, 4H, Ar), 7.41 (ddd, 1H, *J* = 8.0, 8.0, 5.0 Hz, Ar), 3.60−3.52 (m, 2H, CH), 3.10−3.00 (m, 2H, CH), 2.72−2.66 (4H, m, CH), 2.51 (s, 3H, NMe).

Synthesis of 5-Fluoro-2-(4-methylpiperazin-1-yl)-3-(4-(trifluoromethoxy)-phenyl)-quinazolin-4(3*H*)-one (30). (Step A) 5-Fluoro-2*H*-benzo[*d*][1,3]-oxazine-2,4(1*H*)-dione (**45a**)

Triphosgene (1.91 g, 6.45 mmol, 1.0 equiv) was added to a solution of 6-fluoroanthranilic acid **44a** (1.0 g, 6.45 mmol, 1.0 equiv) in THF (20 mL) and stirred at RT for 4 h. After diluting with hexane (20 mL), the reaction mixture was filtered out to collect the precipitate. The precipitate was dried under reduced pressure to give 6-fluoroisatoic

DOI: 10.1021/acs.jmedchem.8b01615
J. Med. Chem. 2019, 62, 1468−1483

anhydride **45a** (821 mg, 70%) as a colorless solid, with MS (ESI) m/z 180 [$(M - H)^+$], RT, 0.82 min.

(Step B) 2-Amino-6-fluoro-*N*-(4-(trifluoromethoxy)-phenyl)-benzamide (**47a**) was prepared from **45a** analogous to the synthesis of **47e** from **45d** to afford **47a** (175 mg, quant) as a colorless solid, with MS (ESI) m/z 315 [$(M + H)^+$], RT, 1.74 min.

(Step C) 5-Fluoro-2-thioxo-3-(4-(trifluoromethoxy)-phenyl)-2,3-dihydroquinazolin -4(1*H*)-one (**48a**) was prepared from **47a** analogous to the synthesis of **48e** from **47e** to afford **48a** (85.3 mg, 94%) as a colorless solid, with MS (ESI) m/z 357 [$(M + H)^+$], RT, 1.59 min.

(Step D) 2-Chloro-5-fluoro-3-(4-(trifluoromethoxy)-phenyl)-quinazolin-4(3*H*)-one (**49a**) was prepared from **48a** analogous to the synthesis of **49e** from **48e** to afford **49a** (61.3 mg, 71%) as a colorless solid, with MS (ESI) m/z 359 [$(M + H)^+$], RT, 1.77 min.

(Step E) 5-Fluoro-2-(4-methylpiperazin-1-yl)-3-(4-(trifluoromethoxy)-phenyl)-quinazolin-4(3*H*)-one (**30**) was prepared from **49a** analogous to the synthesis of **10** from **49e** to afford **30** (29.3 mg, quant) as a colorless solid, ^{1}H NMR (400 MHz, DMSO-d_6) δ 7.70 (ddd, 1H, J = 8.0, 8.0, 5.5 Hz, Ar), 7.60−7.55 (m, 2H, Ar), 7.47 (d, 1H, J = 8.0 Hz, Ar), 7.37 (d, 1H, J = 8.0 Hz, Ar), 7.03 (dd, 1H, J = 10.0, 8.0 Hz, Ar), 3.19 (br t, 4H, J = 5.0 Hz, CH), 2.28−2.17 (m, 7H, CH&NMe); ^{13}C NMR (100.6 MHz, DMSO-d_6) δ 162.95 (C═O), 160.33 (*ipso*-Ar), 154.47 (Ar), 149.95 (Ar), 148.58 (Ar), 135.75 (Ar), 135.22 (*ipso*-Ar), 135.11 (*ipso*-Ar), 130.88 (Ar), 121.78 (Ar), 121.75 (Ar), 121.16 (Ar), 110.03 (*ipso*-Ar), 110.83 (*ipso*-Ar), 53.49 (CH_2), 48.07 (CH_2), 44.49 (CH_3); MS (ESI) m/z 423 [$(M + H)^+$], RT, 1.04 min; purity, 100% (ELSD), 100% (PDA).

Synthesis of 6-Fluoro-2-(4-methylpiperazin-1-yl)-3-(4-(trifluoromethoxy)-phenyl)-quinazolin-4(3*H*)-one (31). (Step A) 6-Fluoro-2*H*-benzo[*d*][1,3]-oxazine-2,4(1*H*)-dione (**45b**) was prepared from **45b** analogous to the synthesis of **45a** from **44a** to afford **45b** (835 mg, 71%) as a colorless solid, with MS (ESI) m/z 180 [$(M - H)^+$], RT, 2.58 min (condition B).

(Step B) 2-Amino-5-fluoro-*N*-(4-(trifluoromethoxy)-phenyl)-benzamide (**47b**) was prepared from **45b** analogous to the synthesis of **47e** from **45d** to afford **47b** (193 mg, quant) as a colorless solid, with MS (ESI) m/z 315 [$(M + H)^+$], RT, 1.72 min.

(Step C) 6-Fluoro-2-thioxo-3-(4-(trifluoromethoxy)-phenyl)-2,3-dihydroquinazolin -4(1*H*)-one (**48b**) was prepared from **47b** analogous to the synthesis of **48e** from **47e** to afford **48b** (36.2 mg, 40%) as a colorless solid, with MS (ESI) m/z 357 [$(M + H)^+$], RT, 1.65 min.

(Step D) 2-Chloro-6-fluoro-3-(4-(trifluoromethoxy)-phenyl)-quinazolin-4(3*H*)-one (**49b**) was prepared from **48b** analogous to the synthesis of **49e** from **48e** to afford **49b** (28.6 mg, 79%) as a colorless solid, with MS (ESI) m/z 359 [$(M + H)^+$], RT, 4.91 min (condition B).

(Step E) 6-Fluoro-2-(4-methylpiperazin-1-yl)-3-(4-(trifluoromethoxy)-phenyl)-quinazolin-4(3*H*)-one (**31**) was prepared from **49b** analogous to the synthesis of **10** from **49e** to afford **31** (18.6 mg, quant) as a colorless solid, ^{1}H NMR (400 MHz, DMSO-d_6) δ 7.75 (dd, 1H, J = 8.0, 3.0 Hz, Ar), 7.65−7.52 (m, 4H, Ar), 7.49−7.44 (m, 2H, Ar), 3.17 (br t, 4H, J = 5.0 Hz, CH), 2.27−2.15 (m, 4H, CH&NMe); ^{13}C NMR (100.6 MHz, DMSO-d_6) δ 162.71 (C═O), 158.69 (*ipso*-Ar), 153.43 (*ipso*-Ar), 148.82 (*ipso*-Ar), 144.54 (Ar), 135.82 (Ar), 130.78 (Ar), 128.39 (Ar), 128.31 (Ar), 123.07 (Ar), 122.83 (Ar), 121.15 (Ar), 111.16 (Ar), 110.93 (Ar), 53.52 (CH_2), 48.29 (CH_2), 44.49 (CH_3); MS (ESI) m/z 423 [$(M + H)^+$], RT, 1.11 min; purity, 100% (ELSD), 100% (PDA).

Synthesis of 7-Fluoro-2-(4-methylpiperazin-1-yl)-3-(4-(trifluoromethoxy)-phenyl)-quinazolin-4(3*H*)-one (32). (Step A) 2-Amino-4-fluoro-*N*-(4-(trifluoromethoxy)phenyl)-benzamide (**47c**) was prepared from **45c** analogous to the synthesis of **47e** from **45d** to afford **47c** (3.0 g, 89%) as a gray solid, with MS (ESI) m/z 315 [$(M + H)^+$], RT, 4.69 min (condition B).

(Step B) 7-Fluoro-2-thioxo-3-(4-(trifluoromethoxy)-phenyl)-2,3-dihydroquinazolin-4(1*H*)-one (**48c**) was prepared from **47c** analogous to the synthesis of **48e** from **47e** to afford **48c** (1.69 g, quant) as a colorless solid, with MS (ESI) m/z 355 [$(M + H)^+$], RT, 1.65 min.

(Step C) 2-Chloro-7-fluoro-3-(4-(trifluoromethoxy)-phenyl)-quinazolin-4(3*H*)-one (**49c**) was prepared from **48c** analogous to the synthesis of **49e** from **48e** to afford **49c** (942 mg, quant) as a colorless solid, with MS (ESI) m/z 359 [$(M + H)^+$], RT, 4.85 min (condition B).

(Step D) 7-Fluoro-2-(4-methylpiperazin-1-yl)-3-(4-(trifluoromethoxy)phenyl)quinazolin-4(3*H*)-one (**32**) was prepared from **49c** analogous to the synthesis of **10** from **49e** to afford **32** (12.9 mg, 50%) as a colorless solid, with ^{1}H NMR (400 MHz, DMSO-d_6) δ 8.15 (dd, 1H, J = 8.0, 3.0 Hz, Ar), 7.61−7.56 (m, 2H, Ar), 7.49−7.44 (m, 2H, Ar), 7.23 (dd, 1H, J = 10.0, 2.5 Hz, Ar), 7.14 (dd, 1H, J = 8.0, 2.5 Hz, Ar), 3.20 (br t, 4H, J = 5.0 Hz, CH), 2.27−2.15 (m, 4H, CH&NMe); ^{13}C NMR (100.6 MHz, DMSO-d_6) δ 162.68 (C═O), 154.85 (*ipso*-Ar), 150.21 (*ipso*-Ar), 148.60 (*ipso*-Ar), 135.93 (Ar), 130.75 (Ar), 129.65 (Ar), 129.54 (Ar), 121.19 (Ar), 115.60 (Ar), 113.17 (Ar), 112.93 (Ar), 110.87 (Ar), 110.65 (Ar), 53.48 (CH_2), 48.15 (CH_2), 44.48 (CH_3); MS (ESI) m/z 423 [$(M + H)^+$], RT, 1.11 min; purity, 100% (ELSD), 100% (PDA).

8-Fluoro-2-(4-methylpiperazin-1-yl)-3-(4-((tetrahydro-2*H*-pyran-4-yl)oxy)-phenyl)-quinazolin-4(3*H*)-one (33). Yield: 4.2 mg, ^{1}H NMR (400 MHz, DMSO-d_6) δ 7.94−7.15 (m, 1H, Ar), 7.55−7.49 (m, 1H, Ar), 7.39−7.35 (m, 2H, Ar), 7.23−7.18 (m, 1H, Ar), 7.16−7.12 (m, 2H, Ar), 4.01−3.93 (m, 4H, CH), 3.66−3.57 (m, 4H, CH), 3.25−3.17 (m, 1H, CH), 2.84 (s, 3H, NMe), 2.11−2.02 (m, 4H, CH), 1.81−1.68 (m, 4H, CH); MS (ESI) m/z 440 [$(M + H)^+$], RT, 0.88 min; purity, 100% (ELSD), 95% (PDA).

3-(4-Benzylphenyl)-8-fluoro-2-(4-methylpiperazin-1-yl)-quinazolin-4(3*H*)-one (34). Yield: 4.1 mg, ^{1}H NMR (400 MHz, DMSO-d_6) δ 7.94 (d, 1H, J = 8.0 Hz, Ar), 7.54 (dd, 2H, J = 8.0, 8.0 Hz, Ar), 7.45 (d, 2H, J = 8.0 Hz, Ar), 7.42−7.20 (m, 9H, Ar), 7.59−7.52 (m, 2H, Ar), 7.39 (ddd, 1H, J = 8.0, 8.0, 5.0 Hz, Ar), 4.09 (br s, 2H, CH_2), 3.79 (br s, 4H, CH), 3.10 (br s, 4H, CH), 2.82 (s, 3H, NMe); MS (ESI) m/z 430 [$(M + H)^+$], RT 1.10 min; purity, 100% (ELSD), 100% (PDA).

8-Fluoro-2-(4-methylpiperazin-1-yl)-3-(4-phenoxyphenyl)-quinazolin-4(3*H*)-one (35). Yield: 3.3 mg, ^{1}H NMR (400 MHz, DMSO-d_6) δ 7.86 (d, 1H, J = 1.5 Hz, Ar), 7.64 (dd, 1H, J = 1.5, 1.5 Hz, Ar), 7.52 (d, 2H, J = 8.0 Hz, Ar), 7.45 (dd, 2H, J = 8.0, 8.0 Hz, Ar), 7.39−7.31 (m, 1H, Ar), 7.23−7.06 (m, 6H, Ar), 6.52 (s, 1H, Ar), 3.31−3.27 (m, 4H, CH), 2.54 (s, 3H, NMe), 2.51−2.47 (m, 4H, CH); MS (ESI) m/z 431 [$(M + H)^+$], RT, 1.14 min; purity, 97% (ELSD), 96% (PDA).

8-Fluoro-3-(4-(4-fluorophenoxy)-phenyl)-2-(4-methylpiperazin-1-yl)-quinazolin-4(3*H*)-one (36). Yield: 9.6 mg, ^{1}H NMR (400 MHz, DMSO-d_6) δ 7.91 (d, 1H, J = 8.0 Hz, Ar), 7.51 (dd, 1H, J = 8.0, 8.0 Hz, Ar), 7.46−7.40 (m, 2H, Ar), 7.35−7.29 (m, 1H, Ar), 7.20−7.09 (m, 6H, Ar), 3.26 (dd, 4H, J = 5.0, 5.0 Hz, CH), 2.28 (dd, 4H, J = 5.0, 5.0 Hz, CH), 2.25 (s, 3H, NMe); ^{13}C NMR (100.6 MHz, DMSO-d_6) δ 164.19 (C═O), 162.19 (C═O), 158.46 (*ipso*-Ar), 158.25 (*ipso*-Ar), 133.37 (*ipso*-Ar), 131.75 (Ar), 124.74 (*ipso*-Ar), 123.61 (Ar), 123.52 (Ar), 122.36 (Ar), 122.24 (Ar), 121.25 (Ar), 121.13 (Ar), 121.06 (Ar), 119.48 (Ar), 117.74 (Ar), 117.51 (Ar), 55.14 (CH_2), 49.66 (CH_2), 46.07 (NMe); MS (ESI) m/z 449 [$(M + H)^+$], RT, 1.20 min; purity, 100% (ELSD), 100% (PDA).

8-Fluoro-3-(4-(4-fluorophenoxy)-phenyl)-2-(4-methylpiperazin-1-yl)-quinazolin-4(3*H*)-one HCl Salt (36·HCl). **36·HCl** was prepared from **36** analogous to the synthesis of **29·HCl** from **29**, affording **36·HCl** (10.8 mg, 99%) as a colorless solid, ^{1}H NMR (400 MHz, DMSO-d_6) δ 7.84 (d, 1H, J = 8.0 Hz, Ar), 7.67−7.62 (m, 1H, Ar), 7.54−7.47 (m, 2H, Ar), 7.38−7.25 (m, 3H, Ar), 7.18−7.10 (m, 4H, Ar), 2.68−2.65 (m, 4H, CH), 2.33−2.31 (m, 4H, CH), 2.30 (s, 3H, NMe).

Preparation of Azides (38a, 38b, 38c, and 38d) for Solid-Phase Synthesis. *2-Azido-3-chlorobenzoic Acid (38a).* $NaNO_2$ (1.71 g, 26.4 mmol, 2.2 equiv) in water (10 mL) was added dropwise to a stirred solution of 2-amino-3-chlorobenzoic acid **37a** (2.06 g, 12 mmol, 1.0 equiv) in 6 M $HCl_{(aq)}$ at 5 °C. After stirring at 0 °C for 4 h, the solvent was filtered out with a glass funnel to give the yellow solid and then the yellow solid was dissolved to NaOAc (23.6 g, 288 mmol, 24 equiv) in water (26 mL). NaN_3 (1.72 g, 26.4 mmol, 2.2 equiv) in water (4 mL) was added to a stirred solution. After stirring at 0 °C for 4 h, the resulting mixture was quenched with concentrated $HCl_{(aq)}$ (5 mL) and the solvent was filtered out. The yellow solid was washed with 6 M $HCl_{(aq)}$ and dried in reduced pressure, to give the azide product

DOI: 10.1021/acs.jmedchem.8b01615
J. Med. Chem. 2019, 62, 1468−1483

38a (2.39 g, 28 %) as a yellow solid, ^{1}H NMR (400 MHz, DMSO-d_6) δ 8.00 (dd, 1H, J = 9.0, 3.0 Hz, Ar), 7.63 (dd, 1H, J = 6.0, 3.0 Hz, Ar), 7.26 (dd, 1H, J = 9.0, 3.0 Hz, Ar); MS (ESI) m/z 196 [$(M - H)^+$], RT, 1.26 min.

2-Azido-3-fluorobenzoic Acid (38b). **38b** was prepared from **37b** analogous to the synthesis of **38a** from **37a** to afford **38b** (1.17 g, 98 %) as a brown solid, ^{1}H NMR (400 MHz, DMSO-d_6) δ 7.89 (ddd, 1H, J = 9.0, 3.0, 3.0 Hz, Ar), 7.39−7.32 (m, 1H, Ar), 7.26−7.18 (m, 1H, Ar); MS (ESI) m/z 180 [$(M - H)^+$], RT, 1.09 min.

2-Azido-3-bromobenzoic Acid (38c). **38c** was prepared from **37c** analogous to the synthesis of **38a** from **37a** to afford **38c** (2.39 g, 28 %) as a yellow solid, ^{1}H NMR (400 MHz, DMSO-d_6) δ 8.04 (dd, 1H, J = 9.0, 3.0 Hz, Ar), 7.82 (dd, 1H, J = 6.0, 3.0 Hz, Ar), 7.18 (dd, 1H, J = 9.0, 9.0 Hz, Ar); MS (ESI) m/z 227 [$(M - H)^+$], RT, 0.27 min.

2-Azido-3-methoxybenzoic Acid (38d). **38d** was prepared from **37d** analogous to the synthesis of **38a** from **37a** to afford **38d** (2.39 g, 28 %) as a yellow solid, ^{1}H NMR (400 MHz, DMSO-d_6) δ 7.78 (dd, 1H, J = 9.0, 3.0 Hz, Ar), 7.21 (dd, 1H, J = 9.0, 9.0 Hz, Ar), 7.10 (dd, 1H, J = 9.0, 3.0 Hz, Ar); MS (ESI) m/z 192 [$(M - H)^+$], RT, 1.08 min.

SOX9 Reporter Gene Assay. The SOX9 reporter gene was previously reported.[17] Human TRPV4 cDNA (NM_021625) was subcloned into the pcDNA3.1 vector. Reporter assays were performed using the stable ATDC5 cell line carrying reporter gene constructs and human TRPV4 expression constructs. Stable cells were inoculated at a density of 2.0×10^4 cells/well in 96-well white plates and treated with an appropriate concentration of compounds. Luciferase activity was measured the next day using a Picagene LT 2.0 luminescence kit (Toyo Ink).

Measurement of Intracellular Ca^{2+}. Cellular Ca^{2+} was estimated using the ratiometric fluorescence Ca^{2+} indicator Fura-2. HEK293 cells transiently expressing human TRPV4 were incubated at 37 °C for 30 min in assay buffer (20 mM HEPES (pH 7.4), 115 mM NaCl, 5.4 mM KCl, 0.8 mM $MgSO_4$, 1.8 mM $CaCl_2$, 13.8 mM glucose, and 0.1% bovine serum albumin), containing 5 μM Fura-2 AM (Dojindo) and 0.2% Pluronic F-127 (molecular probes). The cells were then washed and resuspended in assay buffer. Cellular Ca^{2+} was measured by ratio imaging of Fura-2 fluorescence (emission at 510 nm with excitation at 340 and 380 nm) using a Functional Drug Screening System 3000 (Hamamatsu Pho-tonics).

Normal Human Articular Chondrocyte Cell System Assay. NHAC cells were obtained from Lonza. We evaluated chondrogenesis activity by stimulating the cells for 30 min with TRPV4 agonists, then replacing the medium. After 3 days' culture, the cells were fixed with 95% methanol and stained with 0.1% Alcian blue 8GS (Sigma) in 0.1 N HCl overnight. Alcian blue-stained cultures were extracted with 6 M guanidine−HCl for 2 h at room temperature. The optical density of the extracted dye was measured at 600 nm.

MT Model and Drug Treatment. Eight-week-old Sprague Dawley male rats obtained from Japan SLC were housed one per cage and acclaimed prior to use. All animals were allowed access to food and water ad libitum before and after surgery. The experimental protocols were performed according to relevant national and international guidelines and were approved by the Animal Experimental Ethical Committee. When the rats were 100 weeks old, they were anesthetized with pentobarbital and the right knee was prepared for surgery. A skin incision was made over the medial aspect of the right knee; then, the medial collateral ligament was exposed by blunt dissection and transected. A full-thickness cut was made through the medial meniscus to simulate a complete tear. The muscle and skin were closed with 6-O Vicryl and 4-O Silk suture, respectively. One week after the surgery, the rats were divided into four equal-sized groups by body weight: 1, sham (vehicle); 2, MT (vehicle); 3, MT (5 μM); and 4, MT (10 μM). Next, 50 μL of saline as the vehicle or **36·HCl** solution was injected intra-articularly into the operated knee twice a week for three consecutive weeks. The rats were euthanized at week 4, and the right knee joints were harvested for histological evaluation.

Histology and Evaluation. The knee joints were fixed with 10% neutral buffered formalin and decalcified with 5% formic acid formalin. The decalcified joint was cut to allow observation of the inside and outside articular surface. After dehydration using graded alcohol solutions, each joint was embedded in paraffin, sliced thinly (5 μm), double stained with safranine-O and Fast Green, and then observed under a microscope. Tibial cartilage histopathological evaluation was used to measure cartilage degeneration in three equally spaced regions across the surface of the medial tibial plateau. The score is reported as follows. The term "minimal change" indicates the loss of chondrocytes and proteoglycans with or without fibrillation involving the superficial zone. The term "mild change" means the loss of chondrocytes and proteoglycans with or without fibrillation involving the upper 1/3 of the cartilage thickness. The term "moderate change" means the loss of chondrocytes and proteoglycans, with fibrillation extending well into the mid zone and generally affecting 1/2 of the total cartilage thickness. The term "marked degeneration" means the loss of chondrocytes and proteoglycans, with fibrillation extending into the deep zone but with residual matrix above the tidemark. Finally, the term "severe degeneration" means matrix loss to the tidemark. The scoring method allowed strict attention to the zones (outside, middle, and inside 1/3), and the summed scores reflected the global severity of tibial cartilage degeneration. Significant changes in the width of the cartilage were determined by micrometer measurements of the width of the surface of the tibial plateau. Chondrocyte and matrix losses were evident in more than 50% of the cartilage thickness. The depth ratio, which is the percent of cartilage thickness eroded by a lesion, was determined by micrometer measurements of the depth of all lesions at four equally spaced points on the tibial surface. These measurements were taken at the matrix adjacent to the chondrophyte and at 1/4, 1/2, and 3/4 of the distance across the tibial plateau. The depth to the tidemark was used to express cartilage thickness across the tibial plateau. Chondrophyte size was measured using an ocular micrometer, and the values were averaged for the three sections taken per animal. Bone and calcified cartilage damage were used to evaluate damage to the calcified cartilage and subchondral bone, categorized into six stages:

1 No change.

2 Increased basophilia at the tidemark but no fragmentation of the tidemark and no changes to the marrow.

3 Increased basophilia at the tidemark, with minimal to mild fragmentation of the calcified cartilage.

4 Increased basophilia at the tidemark, with mesenchymal changes that involve up to 3/4 of the total area. In addition, areas of chondrogenesis may be evident but there is no collapse of articular cartilage into the epiphyseal bone.

5 Increased basophilia at the tidemark, with mark to severe fragmentation of the calcified cartilage and mesenchymal changes in the marrow that involve up to 3/4 of the total area. The articular cartilage collapses into the epiphysis to a depth of 250 mm from the tidemark.

6 Increased basophilia at the tidemark with mark to severe fragmentation of the calcified cartilage and mesenchymal changes in the marrow that involve up to 3/4 of the total area. The articular cartilage collapses into the epiphysis to a depth 250 mm from the tidemark.

RNA Isolation and Quantitative Real-Time PCR Analysis. Cartilage tissue was freeze-pulverized in liquid nitrogen followed by RNA extraction using an RNAeasy Lipid Tissue Mini kit (Qiagen) with DNase I (Qiagen) treatment. Total RNA was used to synthesize cDNA using SuperScript III reverse transcriptase (Invitrogen). Quantitative real-time PCR was performed on an ABI Prism 7000 Sequence Detection system using TaqMan Gene Expression Master Mix and TaqMan Gene Expression Assays (Applied Biosystems). Expression values were normalized to ribosomal protein RPL19.

Statistical Analysis. All quantitative data are presented as mean ± standard deviation (SD). Statistical analyses were performed using EXSUS ver. 8.1 (CAC Croit) based on SAS ver. 9.2 (SAS Institute Japan). Comparisons between group-administered vehicle or 5 μM or 10 μM **36·HCl** were performed using Dunnett's test, with the control group as a reference. Differences were considered statistically significant at $p < 0.05$.

DOI: 10.1021/acs.jmedchem.8b01615
J. Med. Chem. 2019, 62, 1468−1483

■ ASSOCIATED CONTENT

Supporting Information

The Supporting Information is available free of charge on the ACS Publications website at DOI: 10.1021/acs.jmedchem.8b01615.

Molecular formula strings and some data (CSV)

Supporting figure as NHAC cell assay with short-term stimulation of **36** (PDF)

■ AUTHOR INFORMATION

Corresponding Author

*E-mail: atobe.mb@om.asahi-kasei.co.jp. Phone: +81-558-76-8493. Fax: +81-558-76-5755.

ORCID

Masakazu Atobe: 0000-0002-7314-0237

Present Address

[⊥]Asahi Kasei Pharma, Diagnostic Department R&D Group, 632-1, Mifuku, Izunokuni, Shizuka, Tokyo 410-2321, Japan (S.M., M.K.). Asahi Kasei Pharma, Open Innovation Department, Hibiya Mitsui Tower, 1-1-2 Yurakucho, Chiyoda-ku, Tokyo 101-0006, Japan (T.O.).

Author Contributions

[▽]M.A. and T.N. contributed equally to this work. The manuscript was written through contributions of all authors. All authors have given approval to the final version of the manuscript.

Notes

The authors declare no competing financial interest.

■ ACKNOWLEDGMENTS

The authors thank Dr. Kenji Takenuki, Yukio Tsuchiya, and Noritsugu Kitahara from the Laboratory for Medicinal Chemistry at Asahi Kasei Pharma Corporation, for conducting the initial chemistry experiments, Dr. Daisuke Shimosato in the Laboratory for Pharmacology at Asahi Kasei Pharma Corporation, for conducting the molecular biology experiments, Toru Kobayashi in the Laboratory for Pharmacology at Asahi Kasei Pharma Corporation, for supporting in vivo experiments, Eiichi Tanaka, Satoshi Shiojiri, and Dr. Akio Matsuda in the Laboratory for Pharmacology at Asahi Kasei Pharma Corporation, for project management support, and Dr. Shunsuke Tahara in the Laboratory for Pharmacology at Asahi Kasei Pharma Corporation, for statistical analysis support.

■ ABBREVIATIONS

ATDC, a murine chondrogenic cell line; DIC, *N*,*N*′-diisopropyl carbodiimide; DIEA, diisopropyl ethylamine; DMEM, Dulbecco's modified Eagle medium; DMSO, dimethyl sulfoxide; EtOH, ethanol; FGF18, fibroblast growth factor 18; GSK, Glaxo Smith Klein; HEPES, 4-(2-hydroxyethyl)-1-piperazineethanesulfonic acid; HTS, high-throughput screening; MT, medial meniscal tear; NHAC, normal human articular chondrocyte; OA, osteoarthritis; 4α-PDD, 4α-phorbol-12,13-didecanoate; PK, pharmacokinetic; POA, primary osteoarthritis; PTOA, post-traumatic osteoarthritis; SAR, structure−activity relationship; SOX, SRY (sex-related Y)-type high-mobility group box; TFA, trifluoroacetic acid; THF, tetrahydrofuran; TRPV4, transient receptor potential vanilloid 4

■ REFERENCES

(1) Mankin, H. J.; Lippiello, L. Biochemical and metabolic abnormalities in articular cartilage from osteoarthritic human hips. *J. Bone Jt. Surg.* **1970**, *52*, 424−434.

(2) Buckwalter, J. A.; Martin, J. A. Osteoarthritis. *Adv. Drug Delivery Rev.* **2006**, *58*, 150−167.

(3) Osteoarthritis - Pipeline Assessment and Market Forecasts to 2017, GlobalData Reference Code: GDHC157PRT, published on Dec, 2010.

(4) Zweers, M. C.; de Boer, T. N.; van Roon, J.; Bijlsma, J. W. J.; Lafeber, F. P.; Mastbergen, S. C. Celecoxib: considerations regarding its potential disease-modifying properties in osteoarthritis. *Arthritis Res. Ther.* **2011**, *13*, 239−249.

(5) Goldring, S. R.; Goldring, M. B. Osteoarthritis. *J. Cell Physiol.* **2007**, *213*, 626−634.

(6) Goldring, S. R.; Goldring, M. B. The role of cytokines in cartilage matrix degeneration in osteoarthritis. *Clin. Orthop. Relat. Res.* **2004**, *427*, S27−36.

(7) Miyamoto, M.; Ito, H.; Mukai, S.; Kobayashi, T.; Yamamoto, H.; Kobayashi, M.; Maruyama, T.; Akiyama, H.; Nakamura, T. Simultaneous stimulation of EP_2 and EP_4 is essential to the effect of prostaglandin E_2 in chondrocyte differentiation. *Osteoarthritis Cartilage* **2003**, *11*, 644−652.

(8) Moore, E. E.; Bendele, A. M.; Thompson, D. L.; Littau, A.; Waggie, K. S.; Reardon, B.; Ellsworth, J. L. Fibroblast growth factor-18 stimulates chondrogenesis and cartilage repair in a rat model of injury-induced osteoarthritis. *Osteoarthritis Cartilage* **2005**, *13*, 623−631.

(9) Otsuka, S.; Aoyama, T.; Furu, M.; Ito, K.; Jin, Y.; Nasu, A.; Fukiage, K.; Kohno, Y.; Maruyama, T.; Kanaji, T.; Nishimura, A.; Sugihara, H.; Fujimura, S.; Otsuka, T.; Nakamura, T.; Toguchida, J. PGE_2 signal via EP_2 receptors evoked by a selective agonist enhances regeneration of injured articular cartilage. *Osteoarthritis Cartilage* **2009**, *17*, 529−538.

(10) Akiyama, H.; Chaboissier, M. C.; Martin, J. F.; Schedl, A.; de Crombrugghe, B. The transcription factor Sox9 has essential roles in successive steps of the chondrocyte differentiation pathway and is required for expression of Sox5 and Sox6. *Genes Dev.* **2002**, *16*, 2813−2828.

(11) Bi, W.; Deng, J. M.; Zhang, Z.; Behringer, R. R.; de Crombrugghe, B. Sox9 is required for cartilage formation. *Nat. Genet.* **1999**, *22*, 85−89.

(12) Lefebvre, V.; Huang, W.; Harley, V. R.; Goodfellow, P. N.; de Crombrugghe, B. SOX9 is a potent activator of the chondrocyte-specific enhancer of the Proα1(II) collagen Gene. *Mol. Cell. Biol.* **1997**, *17*, 2336−2346.

(13) Zhang, P.; Jimenez, S. A.; Stokes, D. G. Regulation of human COL9A1 gene expression Activation of the proximal promoter region by sox9. *J. Biol. Chem.* **2003**, *278*, 117−123.

(14) Bridgewater, L. C.; Lefebvre, V.; de Crombrugghe, B. Chondrocyte-specific enhancer elements in the Col11α2 gene resemble the Col2α1 tissue-specific enhancer. *J. Biol. Chem.* **1998**, *273*, 14998−15006.

(15) Sekiya, I.; Tsuji, K.; Koopman, P.; Watanabe, H.; Yamada, Y.; Shinomiya, K.; Nifuji, A.; Noda, M. SOX9 enhances aggrecan gene promoter/enhancer activity and is up-regulated by retinoic acid in a cartilage-derived cell line, TC6. *J. Biol. Chem.* **2000**, *275*, 10738−10744.

(16) Lefebvre, V.; Ki, P.; de Crombrugghe, B. A new long form of Sox5(L-Sox5), Sox6 and Sox9 are co-expressed in chondrogenesis and cooperatively activate the type II collagen gene. *EMBO J.* **1998**, *17*, 5718−5733.

(17) Muramatsu, S.; Wakabayashi, M.; Ohno, T.; Amano, K.; Ooishi, R.; Sugahara, T.; Shiojiri, S.; Tashiro, K.; Suzuki, Y.; Nishimura, R.; Kuhara, S.; Sugano, S.; Yoneda, T.; Matsuda, A. Functional gene screening system identified TRPV4 as a regulator of chondrogenic differentiation. *J. Biol. Chem.* **2007**, *282*, 32158−32167.

(18) Vennekens, R.; Owsianik, G.; Nilius, B. Vanilloid receptor potential cation channels: An overview. *Curr. Pharm. Des.* **2008**, *14*, 18−31.

DOI: 10.1021/acs.jmedchem.8b01615
J. Med. Chem. 2019, 62, 1468−1483

(19) Nilius, B.; Owsianik, G.; Voets, T.; Peters, J. A. Transient receptor potential channels in disease. *Physiol. Rev.* **2007**, *87*, 165−217.
(20) Vincent, F.; Duncton, M. A. J. TRPV4 agonists and antagonists. *Curr. Top. Med. Chem.* **2011**, *11*, 2216−2226.
(21) Thorneloe, K. S.; Sulpizio, A. C.; Lin, Z.; Figueroa, D. J.; Clouse, A. K.; McCafferty, G. P.; Chendrimada, T. P.; Lashinger, E. S.; Gordon, E.; Evans, L.; Misajet, B. A.; Demarini, D. J.; Na-tion, J. H.; Casillas, L. N.; Marquis, R. W.; Votta, B. J.; Sheardown, S. A.; Xu, X.; Brooks, D. P.; Laping, N. J.; Westfall, T. D. *N*-((1*S*)-1-{[4-((2)-2-{[(2,4-dichlorophenyl)sulfonyl]amino}-3-hydropropanoyl)-1-piperazinyl]-carbonyl}-3-methylbutyl)-1-benzothiophene-2-carboxamide (GSK1016790A), a novel and potent transient receptor potential vanilloid 4 channel agonist induces urinary bladder contraction and hyperactivity: Part I. *J. Pharmacol. Exp. Ther.* **2008**, *326*, 432−442.
(22) Kumar, S.; Pratta, M. A.; Votta, B. J. Method for Activating TRPV4 Channel Receptors by Agonists, WO2006029209 A2, March 16, 2006.
(23) Wilette, R. N.; Bao, W.; Nerukar, S.; Yue, T. L.; Doe, C. P.; Stankus, G.; Turner, G. H.; Ju, H.; Thomas, H.; Fishman, C. E.; Sulpizio, A.; Behm, D. J.; Hoffman, S.; Lin, Z.; Lozinskaya, I.; Casillas, L. N.; Lin, M.; Trout, R. E.; Votta, B. J.; Thorneloe, K.; Lashinger, E. S.; Figueroa, D. J.; Marquis, R.; Xu, X. Systemic activation of the transient receptor potential vanilloid subtype 4 channel causes endothelial failure and circulatory collapse: Part 2. *J. Pharmacol. Exp. Ther.* **2008**, *326*, 443−452.
(24) Watanabe, H.; Vriens, J.; Suh, S. H.; Benham, C. D.; Droogmans, G.; Nilius, B. Heat-evoked activation of TRPV4 channels in a HEK293 cell expression system and in native mouse aorta endothelial cells. *J. Biol. Chem.* **2002**, *277*, 47044−47051.
(25) The concentration on top of the peak.
(26) Due to a stability issue of -SCF_3 group against chlorination step with SO_2Cl_2, -OCF_3 was chosen for rapid fluorine scanning strategy.
(27) Iwase, Y.; Tsutsui, N. HL-60 ATP Assay for Predicting Rat Oral Toxicity Study, *Proceedings of the 6th World Congress on Alternatives & Animal Use in the Life Sciences*, August 21−25, **2007**, Tokyo, Japan, AATEX 14, Special Issue; pp 699−703.
(28) Document # TS-CC-112-6 01/14; www.lonza.com (accessed Jan 5, 2019).
(29) Snowden, J. M.; Maroudas, A. The distribution of serum albumin in human normal and degenerate articular cartilage. *Biochim. Biophys. Acta, Gen. Subj.* **1976**, *428*, 726−740.
(30) Kuyinu, E. L.; Narayanan, G.; Nair, L. S.; Laurencin, C. T. Animal models of osteoarthritis: classification, update, and measurement of outcomes. *J. Orthop. Surg. Res.* **2016**, 11−19.
(31) Janusz, M. J.; Bendele, A. M.; Brown, K. K.; Taiwo, Y. O.; Hsieh, L.; Heitmeyer, S. A. Induction of osteoarthritis in the rat by surgical tear of the meniscus; inhibition of joint damage by a matrix metalloproteinase inhibitor. *Osteoarthritis Cartilage* **2002**, *10*, 785−791.
(32) Lampropoulou-Adamidou, K.; Lelovas, P.; Karadimas, E. V.; Liakou, C.; Triantafillopoulos, I. K.; Dontas, I.; Papaioannou, N. A. Useful animal models for the research of osteoarthritis. *Eur. J. Orthop. Surg. Traumatol.* **2014**, *24*, 263−271.
(33) McCoy, A. M. Animal models of osteoarthritis: comparisons and key considerations. *Vet. Pathol.* **2015**, *52*, 803−818.
(34) Piskin, A.; Gulbahar, M. Y.; Tomak, Y.; Gulman, B.; Hokelek, M.; Kerimoglu, S.; Koksal, B.; Alic, T.; Kalbak, Y. B. Osteoarthritis models after anterior cruciate ligament resection and medial meniscectomy in rats. A histological and immune-histochemical study. *Saudi Med. J.* **2007**, *28*, 1796−1802.
(35) Bove, S. E.; Laemont, K. D.; Brooker, R. M.; Osborn, M. N.; Sanchez, B. M.; Guzman, R. E.; Hook, K. E.; Juneau, P. L.; Connor, J. R.; Kilgore, K. S. Surgically induced osteoarthritis in the rat results in the development of both osteoarthritis-like joint pain and secondary hyperalgesia. *Osteoarthritis Cartilage* **2006**, *14*, 1041−1048.
(36) Bendele, A. M. Animal models of osteoarthritis in an era of molecular biology. *J. Musculoskelet. Neuronal. Interact.* **2002**, *2*, 501−503.
(37) Bendele, A.; McComb, J.; Gould, T.; McAbee, T.; Sennello, G.; Chilipala, E.; Guy, M. Animal models of arthritis: relevance to human disease. *Toxicol. Pathol.* **1999**, *27*, 134−142.
(38) Galois, L.; Etienne, L.; Watrin-Pinzano, A.; Cournil-Henrionnet, D.; Loeuille, P.; Netter, D.; Gillet, P.; et al. Dose-response relationship for exercise on severity of experimental osteoarthritis in rats: a pilot study. *Osteoarthritis Cartilage* **2004**, *12*, 779−786.
(39) Kesarwani, A. P.; Srivastava, G. K.; Rastogi, S. K.; Kundu, B. Solid-phase synthesis of quinazolin-4(3*H*)-ones with three-point diversity. *Tetrahedron Lett.* **2002**, *43*, 5579−5581.
(40) Villalgordo, J. M.; Obrecht, D.; Chucholowsky, A. Solid-phase synthesis of 3H-Quinazoli-4-ones based on an aza Wittig-mediated annulation strategy. *Synlett* **1998**, 1405−1407.
(41) e-DOMINO is a Device Composed of Syringe Manifold, Solenoid Valves, and a Programmable Processor Enabling Automatic Control of Washing Sequences. e-DOMINO is Customized Version of Resin Washer; https://kawadenlab.web.fc2.com/ (accessed Jan 5, 2019) with Additional Valves.
(42) Green, D. E.; Percival, A. Fungicidal Azole Compounds, US Patent 4731106, March 15, 1988.

DOI: 10.1021/acs.jmedchem.8b01615
J. Med. Chem. 2019, 62, 1468−1483